

ACTIVE SHIELDING CONCEPTS FOR THE IONIZING RADIATION IN SPACE

prepared for

NATIONAL AERONAUTICS AND SPACE ADMINISTRATION

by

R.C. GOOD, S.P. SHEN, AND N.F. DOW

Contract NASw-502

Final Report

Rev. 31 Jan. 1964

N64-31552

(ACCESSION NUMBER)

94

(PAGES)

02-58950

(NASA CR OR TMX OR AD NUMBER)

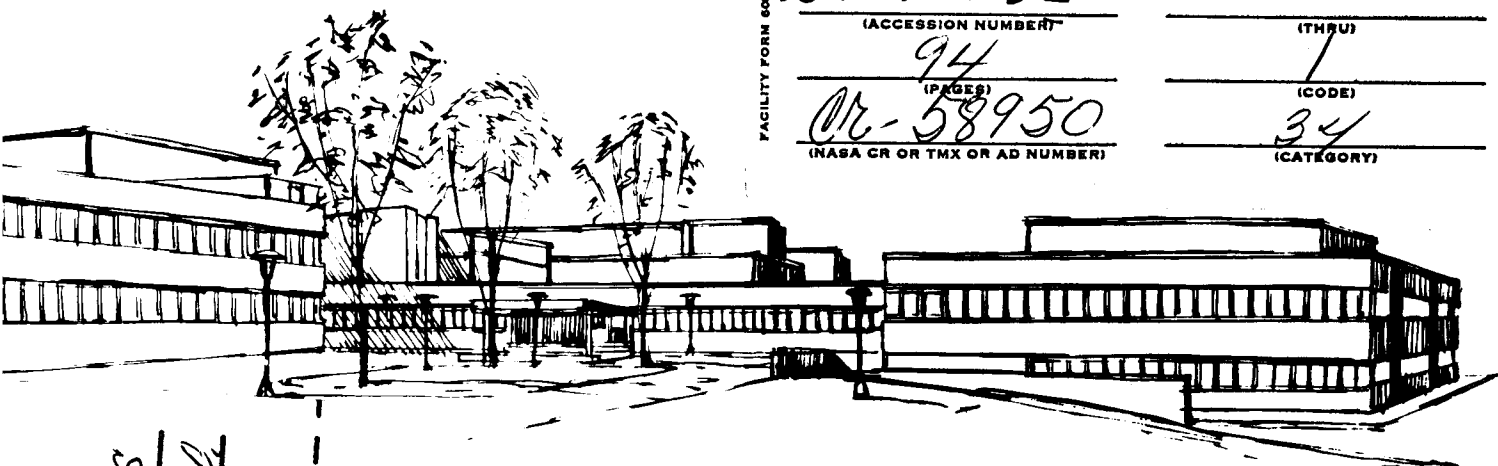
(THRU)

1

(CODE)

34

(CATEGORY)



OTS PRICE

XEROX

\$

3.00 FS

MICROFILM

\$

0.50 mfr

Space Sciences Laboratory
Missile and Space Division
GENERAL ELECTRIC COMPANY
Philadelphia, Pa.

ACTIVE SHIELDING CONCEPTS FOR THE IONIZING RADIATION IN SPACE

Prepared for

National Aeronautics and Space Administration

Prepared by

R. C. Good, S. P. Shen, and N. F. Dow
Space Sciences Laboratory

Final Report

Contract NASw-502

Period Covered: 1 Sept. 1962 - 31 Aug. 1963

Revised January 31, 1964

Missile and Space Division
General Electric Company
P. O. Box 8555, Philadelphia 1, Pennsylvania

Foreword

This report summarizes the work done by the Space Structures Operation of the Space Sciences Laboratory for the National Aeronautics and Space Administration on Contract NASw-502 entitled "Active Shielding Concepts for the Ionizing Radiations in Space." Norris Dow of the Space Sciences Laboratory and S. P. Shen of New York University were consultants on this project. The nuclear cascade experiments were supported in part by the Geophysical Directorate of the Air Force Cambridge Research Laboratories.

Summary

Studies have been made on the problems of shielding a spacecraft from ionizing radiation. Protons having energies between 100 and 1,000 MeV were taken as the radiation that should be excluded from the spacecraft's crew. An electromagnetic field system using a toroidal shaped spacecraft with a confined magnetic field is shown to be the lightest among those treated.

Weight calculations were made for spacecraft having crew spaces of 10, 100, 1,000, and 10,000 cu. ft. Spheres, cylinders, toruses, and spherical modules were selected for crew space configurations. Confined magnetic fields surrounded each with passively shielded hatches added for passageway through the field. The weights were compared with a polyethylene passive shield by plotting the weight of shield system per unit volume of crew space against the Loading Index, the ratio of stopping power to a dimension of the system. Weights of hatch, superconducting coils, thermal insulation, and structural support were calculated.

In general, the active shield weight is only 20% that of the passive shield for high energy protons and for large sizes of spacecraft. The shield with a confined field weighs 30% of that for a shield using an unconfined field. If hatches are included, the use of spherical modules leads to spacecraft that are lighter than spheres, cylinders, or toruses. For spacecraft in the shape of a torus, a passively shielded hatch is not required because there are no junctions between oppositely directed magnetic fields. In that case, a spacecraft in the shape of a torus is lighter than the other shapes.

Material costs have been estimated for electromagnetic confined field shielding systems using niobium zirconium superconducting wires. These costs are higher than those for a polyethylene shield although at the high proton energies and for large spacecraft they will be comparable when the price of superconductors is reduced by a factor of ten. The weight advantage using niobium tin rather than niobium zirconium is shown to be a factor of two to three. Prices of niobium tin are not commercially quoted for large lots, at present.

Experiments with nuclear cascades produced by proton bombardment of iron, chondrites, and plexiglass have shown a critical depth required for passive shields. The flux intensity of cascade products dangerous to a human body increases to a maximum, then falls off with depth below the irradiated surface. Thus, a thin shield is worse than none at all. An explanation is presented for the nuclear cascade process which governs the variation of flux with distance. This explanation has not been refuted by any experimental data gathered to-date.

The following recommendations are presented: to improve the manufacturing techniques of superconducting wire, to study active shielding systems involving combinations of confined and unconfined magnetic fields, to measure nuclear cascades produced by protons with energies below one GeV, to measure secondaries produced by cascades in superconducting material, and to design a prototype model for an experimental feasibility study of a confined space electromagnetic shielding system.

Table of Contents

| | | <u>Page</u> |
|------|---|-------------|
| | Foreword | i |
| | Summary | ii |
| | Table of Contents | iv |
| | List of Figures | vi |
| | List of Tables | viii |
| I. | Introduction | 1 |
| | A. History of Radiation Shielding | 1 |
| | B. Concepts of Shielding | 2 |
| | C. Scope of this Report | 3 |
| II. | Magnetic Field Shielding | 5 |
| | A. Particle Trajectory | 5 |
| | B. Unconfined Fields | 7 |
| | C. Confined Fields | 12 |
| | D. Magnetic Field in the Crew Space | 19 |
| III. | Vehicle Considerations | 23 |
| | A. Basic Assumptions | 23 |
| | B. Spacecraft Configurations | 25 |
| | C. Hatch Construction | 30 |
| | D. Structural Requirements | 31 |
| | E. Magnetic Field Engineering | 33 |
| IV. | Optimization Procedures | 38 |
| | A. Possible Criteria (weight, size, cost) | 38 |
| | B. Weight Calculations | 41 |
| | C. Structural Weight | 54 |
| | D. Superconductor Wire Coils | 56 |
| | E. Cost Calculations | 58 |

| | <u>Page</u> |
|------------------------------------|-------------|
| V. Passive Shielding | 60 |
| A. Introduction | 61 |
| B. Nuclear Cascade Experiments | 62 |
| C. Qualitative Cascade Description | 68 |
| VI. Results & Conclusions | 76 |
| VII. Recommendations | 80 |
| Bibliography | 81 |

List of Illustrations

| | <u>Page</u> |
|---|-------------|
| Figure 1a Coordinate System for Magnetic Dipole | 9 |
| 1b Trajectory in the Equatorial Plane of a Dipole | 9 |
| 2 Forbidden Regions for Particles Approaching a Dipole | 10 |
| 3 Confined Magnetic Field | 15 |
| 4a Trajectory of Particles in a Magnetic Field | 17 |
| 4b Dimensions for Determining the Depth of the Confined Magnetic Field | 18 |
| 5 Sketch of Single Turn Coil Radiation Shield | 21 |
| 6 Principle of Proton Leaks | 26 |
| 7 Preliminary Sketch of Magnetic Shielding Configuration for a Sphere | 27 |
| 8a Torus Cross Section | 29 |
| 8b Junction of Magnetic Field Spaces | 29 |
| 9 Field Smoothing Coils to Alleviate Radial Variation | 37 |
| 10 Spherical Shape Weight Optimization | 40 |
| 11 Comparison of Shielding Weights | 45 |
| I - Sphere, Cylinder, Polyethylene | |
| 12 Comparison of Shielding Weights | 50 |
| II - Sphere, Cylinder, Torus, Polyethylene | |
| 13 Schematic Diagram of Spherical Modules | 52 |
| 14 Comparison of Shielding Weights | 53 |
| III - Sphere, Cylinder, Module, Polyethylene | |

| | <u>Page</u> |
|--|-------------|
| 15 Comparison of Shielding Weights | 55 |
| IV - Confined vs. Unconfined Magnetic Fields | |
| 16 Typical Target Assembly | 64 |
| 17 Transition Curves for the Fluxes of "N" and "n" | 65 |
| 18 Some Idealized Transition Curves | 67 |
| 19 Schematic Representation of the Nuclear Cascade | 70 |

List of Tables

| | <u>Page</u> |
|--|-------------|
| I. Properties of Superconductors | 24 |
| II. Passive Shield Materials for the Hatch | 30 |
| III. Magnetic Field Depths | 41 |
| IV. Radiation Shield Weights, Cylindrical Shape | 42 |
| V. Magnetic Shielding Structure Weights for Spherical Shaped Spacecraft | 46 |
| VI. Magnetic Shield Structure Weights - Torus with Hatch | 48 |
| VII. Magnetic Shield Structure Weights - Torus without Hatch | 49 |
| VIII. Wire Lengths and Stopping Power | 54 |
| IX. Modular Type Spacecraft Weight/Unit Volume Variation of Superconducting Wire | 57 |
| X. Material Cost-Weight Relations for Toroidal Configuration without a Hatch | 59 |
| XI. Nuclear Cascade Experiments | 63 |
| XII. Classification of Secondaries from Inelastic Nuclear Interactions | 69 |

I. Introduction

A. History of Radiation Shielding

The present emphasis in space exploration involves the use of manned spacecraft. From experiments with unmanned satellites, the radiation environment above the earth's atmosphere has been found to be injurious to man in particular regions and lethal to man at certain times.^(1, 2) Thus, we know that manned spacecraft for long space missions must be shielded from the ionizing radiation in space. Since the extent of shielding is still being discussed, activity in this field is presently restricted to conceptual studies of shielding principles and methods.⁽³⁾

There are three sources of ionizing particles which would be encountered by a spacecraft: Galactic cosmic rays, Solar cosmic rays, and geomagnetically trapped radiation.⁽⁴⁾ The first two have been known for some time from sea level and balloon measurements, but even the existence of the last was not demonstrated before 1958 when Explorer I measured part of the flux present. Because the last is the most intense penetrating radiation flux now known to be present in space, every effort must be made to either shield man from this flux or to provide minimal shielding for his passage through the Van Allen belts.⁽⁵⁾

New experiments provide data on the fluxes present that are injurious to man. Summaries have been published at intervals to present the latest data.^(2, 5) Electrons,⁽⁶⁾ protons, and heavier nuclei have been

(1) References are given in the Bibliography

counted in space. At the same time the biologists have been determining the damage to man from ionizing radiation. By combining these two sets of data - the intensity and type of space environment by the space probes and the relative biological effectiveness of the radiation by the biologists - the dosage can be calculated for various trips for space. Keller⁽³⁾ has estimated the space radiation environment and the radiation tissue dose for a point detector located at the center of a spherical shield as a function of shield thickness for several mission categories including high- and low-thrust interplanetary missions of two to three years duration, and for vehicles orbiting in the Van Allen belt for a period of one year. For the interplanetary missions, 10 gm/cm^2 will reduce the dose to a few hundred rem* in the high-thrust case, $80\text{-}100 \text{ gm/cm}^2$ are required to accomplish a similar reduction in the low-thrust case. For manned orbital vehicles operating at altitudes between ~ 900 and 7500 kilometers the Van Allen belt protons are of a magnitude so as to require thick shields for single crew occupancy of one year duration. The required shielding is quite sensitive to the altitude, $40\text{-}160 \text{ gm/cm}^2$ being required to reduce the dose to a few hundred rem depending upon the orbit altitude and inclination.

The above estimates indicate that thick shields may be required for manned spacecraft. If 50 gm/cm^2 of shielding material covered a three meter

* A rem (Roentgen Equivalent Man) is that amount of ionizing radiation of any type which produces the same damage to man as one Roentgen of 200 KV X radiation ($1 \text{ rem} = 1 \text{ rad in tissue} \times \text{RBE}$).

sphere, the shield would weigh about fifteen tons. This weight is out of reason with the present boosters so that it will be necessary to find a lighter shield. This report represents an effort to find the optimum weight for an active shield using electromagnetic fields. ✓

B. Concepts of Shielding

The simplest shield is an umbrella; that is, a mass of material impenetrable to the incoming particles.⁽⁸⁾ Use of this type of device is called passive shielding. There are two major reasons why the simplest may not be the best: (1) the shield stops the incident particles but produces secondaries which are just as bad as the primaries,⁽⁹⁾ or (2) the shield makes the vehicle too cumbersome (too big, too weighty, or too costly) to accomplish its mission.⁽¹⁰⁾

Other methods which deflect the particles away from the spacecraft are called active shields. Several forms have been proposed of which the electrostatic fields have been shown to be useless, permanent magnets to be too heavy, and electromagnets to be of value only if superconductors are used in their coils. In following up this lead, some investigators have studied unconfined magnetic fields such as that produced by a dipole,^(11,12,32) and others have studied confined fields such as are produced by toroidal coils.^(8,10) This report will discuss spacecraft calculations using confined fields. ✓

Shields must be omnidirectional for at least two reasons: (1) the velocity of the spacecraft is diminishingly small compared to that of the particles, and (2) even the solar cosmic rays which stream out from the sun probably become iso-

tropic soon after being emitted at the at the sun's surface.⁽⁴⁾ Because the radiation is isotropic, shields must protect the crew from particle fluxes arriving from any direction which condition makes active shields more difficult to design.

C. Scope of this Report

The above summary shows that shields are required. It is thus prudent for numbers to be obtained which show whether any given configuration or any given shielding structure is an optimum. They form the first basis for actually designing the spacecraft. Some of those calculations are reported below.

The work covered by this report may be broken down into four topics: (a) Theoretical calculations of magnetic fields and their effects on the trajectory of incident particles, (b) Determination of coil design factors (size, position, material, and support) for various shapes of spacecraft (cylindrical, spherical and toroidal), (c) Calculations of the weights for the configurations determined in (b) and selection of the optimum values considering the weight, supporting structure, and type of superconducting material, and (d) Calculation of cascading effects of protons in iron, lucite, and chondrites. A section follows in which the results and conclusions are drawn together from which the final section on recommendations is developed.

II. Magnetic Field Shielding

With the decision to use a magnetic field as the active shielding system, the relations among field, proton velocity, and initial conditions must be determined for uniform magnetic fields, dipole fields, and confined fields. The simpler formulae will be mentioned before the more complicated formulae. Particle trajectories and the restrictions thereon will be derived theoretically. The results will then be used to determine the required size of the confined field to protect the crew space.

A. Particle Trajectory

All formulae are derived from the basic equation of motion for particles of mass, m , and charge ze ,

$$\frac{d}{dt}(m\vec{v}) = \frac{ze}{c} [\vec{E} + \vec{v} \times \vec{B}] \quad (1)$$

where t is the time, \vec{v} the velocity vector, c the velocity of light, \vec{E} the electric field vector, and \vec{B} the magnetic field vector. (All units are given in the cgs system.) In the magnetic field shielding

$$\vec{E} = 0 \quad (2)$$

If particles are traveling perpendicularly to the magnetic field, the acceleration may be set equal to the centripetal acceleration so that the Larmor radius may be given by

$$R_L = \frac{m c v}{ze B} \quad (3)$$

From this one can find the extent ($2 R_1$) of a uniform field B needed to reverse the direction of the worst case trajectory. Thus, the size of a contained magnetic field is obtained for a unidirectional flux of particles having their velocity $\leq v$.

One notes that this expression is valid for constant fields B and for any velocity of particle if the mass, m, is replaced by the relativistic mass

$m_0 / \sqrt{1 - v^2/c^2}$ in which m_0 is the rest mass. Thus

$$R_1 = \frac{m_0 c v}{ze B \sqrt{1 - v^2/c^2}} \quad (4)$$

For cases in which the particle does not strike the field perpendicularly, equation (4) must be multiplied by sine ψ which is the angle between the velocity and field vectors. This force equation may be used for the simpler fields and trajectories.

There are cases where the field is not constant either in magnitude or direction. For these cases the energy approach is more fruitful. Stoermer⁽¹²⁾ originally gave the solution in terms of the vector potential of the magnetic field. The Lagrangian is used for the electromagnetic terms as

$$\mathcal{L} = -m_0 c^2 \sqrt{1 - v^2/c^2} + \frac{ze}{c} \vec{v} \cdot \vec{A} \quad (5)$$

where $\vec{v} \cdot \vec{A}$ is the "dot" product of the velocity with the magnetic vector potential \vec{A} . Equations such as

$$\frac{d}{dt} \left(\frac{\partial \mathcal{L}}{\partial \dot{x}_i} \right) - \frac{\partial \mathcal{L}}{\partial x_i} = 0 \quad (6)$$

are set up for the space variables x_i (x, y, z or ρ, ϕ, z or ρ, λ, ϕ as cartesian, cylindrical, or spherical coordinates).

For a dipole field

$$\bar{A} = \frac{M \cos \lambda}{\rho^2} \hat{e}_\phi \quad (7)$$

where M is the dipole moment, λ is the latitude, and \hat{e}_ϕ is the unit vector in the west direction.

For a toroidal field

$$\bar{A} = -\frac{2NI}{10} \ln \rho \hat{e}_z \quad (8)$$

where NI is the number of ampere turns in the coil, \ln is the natural logarithm, and \hat{e}_z is the unit vector perpendicular to the plane of the coil.

For a single plane coil

$$\bar{A} = \frac{4I}{10k} \sqrt{\frac{a}{\rho}} \left[\left(1 - \frac{k^2}{2}\right) K(k) - E(k) \right] \hat{e}_\phi \quad (9)$$

where a is the radius of the coil, k is the argument of the elliptic integral K of the first kind, $E(k)$ is the elliptic integral of the second kind, and

$$k = \frac{4ap}{(a+\rho)^2 + z^2} \quad (10)$$

all in the cylindrical coordinate system ρ, ϕ, z .

B. Unconfined Fields

The trajectories of particles have been found to have forbidden regions of space when the differential equations (6) are solved. In fact, for the case of

a dipole, only the equation in ϕ needs to be solved. Fermi⁽¹³⁾ plots the regions for several values of the original miss distance. Figure 1a shows the relations of the unit vectors, Figure 1b shows the trajectory and the original miss distance, and Figure 2 shows the forbidden regions. These figures are obtained by setting equation (7) in (5) and solving the equation in the dimension ϕ . The result is

$$R \cos \lambda \cos \gamma + \frac{\cos^2 \lambda}{R} = b \sqrt{\frac{P}{M}} \quad (11)$$

in which R is a dimensionless quantity given by

$$R = \rho \sqrt{\frac{M}{P}} \quad (12)$$

in which P is the magnetic rigidity

$$P = \left| \frac{pc}{Ze} \right| \quad (13)$$

and p is the momentum of the particle. Since γ is the angle between the velocity vector and the west direction its cosine must lie between -1 and +1. Thus, equation (11) is limited and spherical plots of R vs λ have regions that are forbidden.

Suffice it to say that for a space to be protected it should occur in all the diagrams of Figure 2. As the parameter increases from $-\infty$ to +2 the small protected region represented by $\cos \lambda = -1$ shrinks in size. However, at the value of 2 the outer jaws close and the region is now protected by another forbidden region. Thus, the region about the axis that is always shielded is

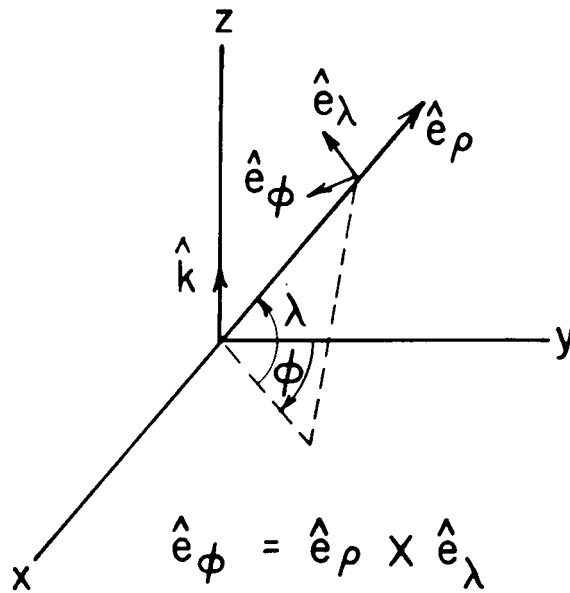


Figure 1a. Coordinate System for Magnetic Dipole

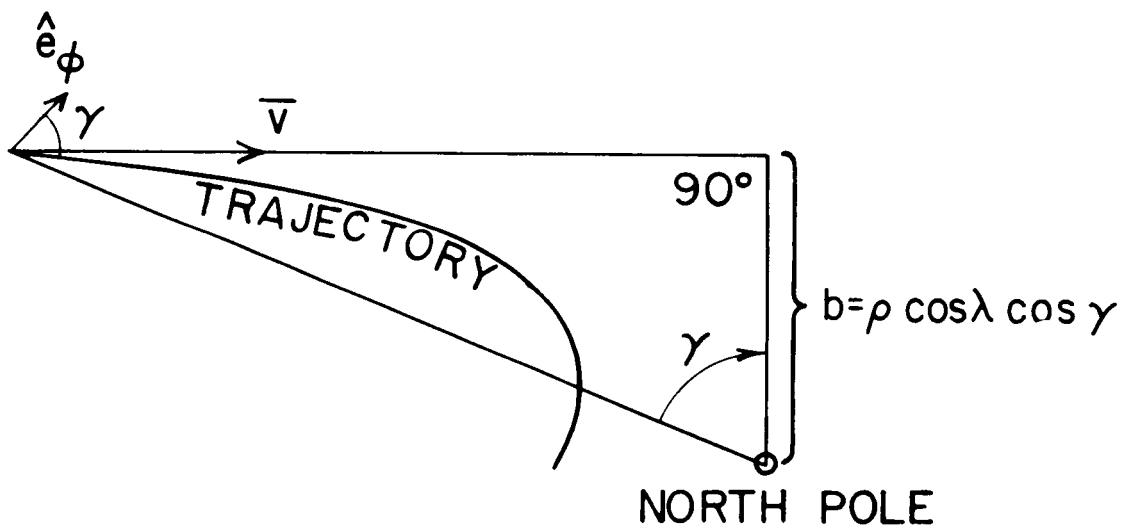
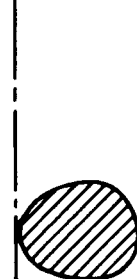
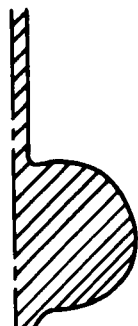
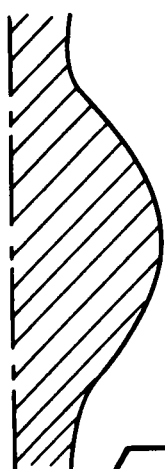


Figure 1b. Trajectory in the Equatorial Plane of a Dipole

$$b\sqrt{\frac{P}{M}} = -0.4$$

$$b\sqrt{\frac{P}{M}} = -0.06$$

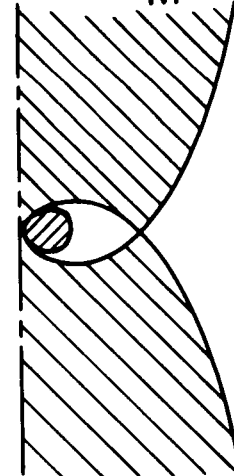
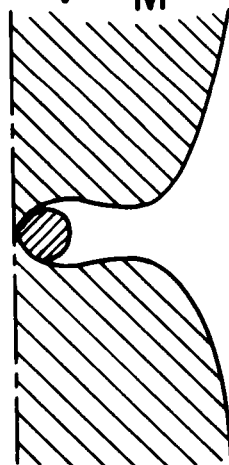
$$b\sqrt{\frac{P}{M}} = 0$$



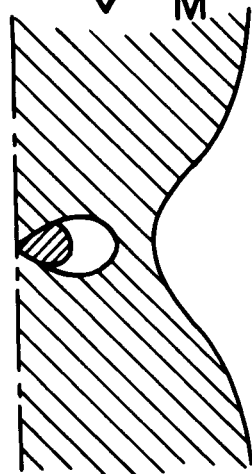
$$b\sqrt{\frac{P}{M}} = 1$$

$$b\sqrt{\frac{P}{M}} = 1.94$$

$$b\sqrt{\frac{P}{M}} = 2$$



$$b\sqrt{\frac{P}{M}} = 2.032$$



CROSS HATCHED AREAS ARE
FORBIDDEN REGIONS

FIGURES ARE SYMMETRIC ABOUT
CENTER LINES

Figure 2. Forbidden Regions for Particles Approaching a Dipole

found by solving equation (11) with the parameter set equal to two and the $\cos \lambda$ set equal to minus one. The radius of that region is 0.414. Any vehicle placed inside the torus will be protected from particles having a momentum equal to or less than the value dictated by the magnetic moment of the dipole.

For example, a vehicle having a one hundred cuft. crewspace in the shape of a torus with a ratio of 4/1 between the two radii would require a dipole moment of 9×10^{11} ergs/gauss. If the dipole were created by single turn coil surrounding the torus, the superconductor required would be eleven centimeters thick and the current would be 1.64×10^8 amperes. It should be noted that if the coil forming the dipole is as large as the forbidden zone, that the dipole approximation does not hold.

The vector potential \bar{A} of a dipole shown in equation (7) is the same as that of a plane coil given in equation (9) only if the point of observation is far from the coil. As the point of observation approaches the coil the direction and magnitude of the field is markedly different. Thus, equation (5) must be solved anew for the proper vector potential of the coil. The equation equivalent to equation (11) is

$$b = r \cos \lambda \cos \gamma + \frac{4I}{10P} r \cos \lambda \sqrt{\frac{a^2 + 2ar \cos \lambda + r^2}{4r^2 \sin \lambda \cos \lambda}} \left[\left(1 - \frac{2ar \cos \lambda}{a^2 r^2 + 2ar \cos \lambda} \right) K(k) - E(k) \right] \quad (14)$$

in which the spherical coordinates of Figure 1a are used. We note the presence of the cosine of gamma to indicate the forbidden regions. Since equation (14) can not be readily solved for r or λ , solutions represented for various versions of b must be obtained by calculations using different values for r , λ , γ , and I/P . As expected, the current in the coil is directly related to the

momentum or the energy of the incident particles from which shielding is desired.

C. Confined Fields

In this case the particles are not expected to deviate from their paths until they enter the confined field. Hence, the fields must be large in magnitude or else extensive in volume. Since the magnitude of the field is limited in practice, it remains to calculate the volume of the space in which the field is to be confined.

In view of the magnitudes of fields required, it is obvious that superconductors will be used to minimize the power needs.

Superconductors are a class of materials which have a drop in resistivity of about sixteen orders of magnitude when their temperature is decreased below a certain critical level. Roberts⁽¹⁴⁾ lists over 500 elements and compounds with their critical temperatures. Experimental determinations of the processes involved are still being carried out. Theories indicate that filaments within the metal structure carry the bulk of the current. Thus, the material becomes superconducting at higher temperatures if these filaments are developable, and the search for materials has been for those having higher critical temperatures. The highest to date is near 19°K.

A second feature of the superconductors is the magnetic fields associated with the currents. The Meissner effect describes the exclusion of magnetic fields from current carrying superconductors. Associated with this concept

is the critical value of magnetic field which the superconductor can no longer exclude. At that value the superconductor ceases to have the necessary properties and "goes" normal. The relation between critical current and critical magnetic field is determined for each material experimentally. Those with the largest critical values of both field and current are judged to be the best.

The data for current and field are roughly hyperbolic in the center of their ranges. Kunzler⁽¹⁵⁾ gives data as of 1961 that has since been surpassed by heat treatments and specialized wire formation. Cladding increases the properties, for example.⁽¹⁶⁾ For the purposes of the work covered by this report, we have used the relation

$$BJ = 6 \times 10^9 \text{ gauss amperes/cm}^2 \quad (15)$$

which is valid for Nb₃Sn in wires of 15 mil diameter. With B taken as 10⁵ gauss (the critical field is extrapolated to 2 x 10⁵ gauss) the current density is set at 6 x 10⁴ amperes/cm². If large currents are required, the cross section of the wire is increased or the number of turns is increased as required. It should be noted that the field is not increased without bound as turns are added to the coil because the inside turns reach a critical field that is smaller than for single turn coils.^(17, 18) However, a coil has been constructed in which the field was measured as 10⁵ gauss.⁽¹⁹⁾ Thus, it will be a matter of increasing technical competence to find a means to build the large coils.

Confined fields are expected to surround the spacecraft much like a hollow cylinder would surround a second cylinder. (For the purpose of the following

description the ends of the cylinder are left open. The space between the cylinders forms a torus. When the coil is wound as a helix about the torus, the field is confined within the torus. Also, the field is dependent upon the current in the coil, the number of turns on the coil, and the distance from the axis of the torus. Thus

$$B = \frac{2NI\mu}{10R_0} \quad (16)$$

where μ is the magnetic permeability which is 1 in air or a vacuum. Figure 3 shows the relations described above. If the wires are square, of a thickness T , and wound as closely as possible in a single layer, the number of turns will be

$$N = \frac{2\pi R_0}{T} \quad (17)$$

so that equation (15) becomes with the current density J for a square wire

$$B = \sqrt{4\pi 6 \times 10^9 T} \quad (18)$$

If the outside radius of the torus is not very different from the inside radius, B will be nearly constant in the confined field. In that case equation (3) or (4) will be applicable and the radius of curvature becomes

$$R_1 = \frac{m c v}{z e \sqrt{24\pi T 10^9}} \quad (19)$$

Since most of the particles treated will be relativistic, equation (19) must have a relativistic mass as m . Then, using the particle energy instead of its velocity,

$$R_2 = \frac{\sqrt{E_p} \sqrt{E_p + 2m_0 c^2}}{z e \sqrt{24\pi T 10^9}} \quad (20)$$

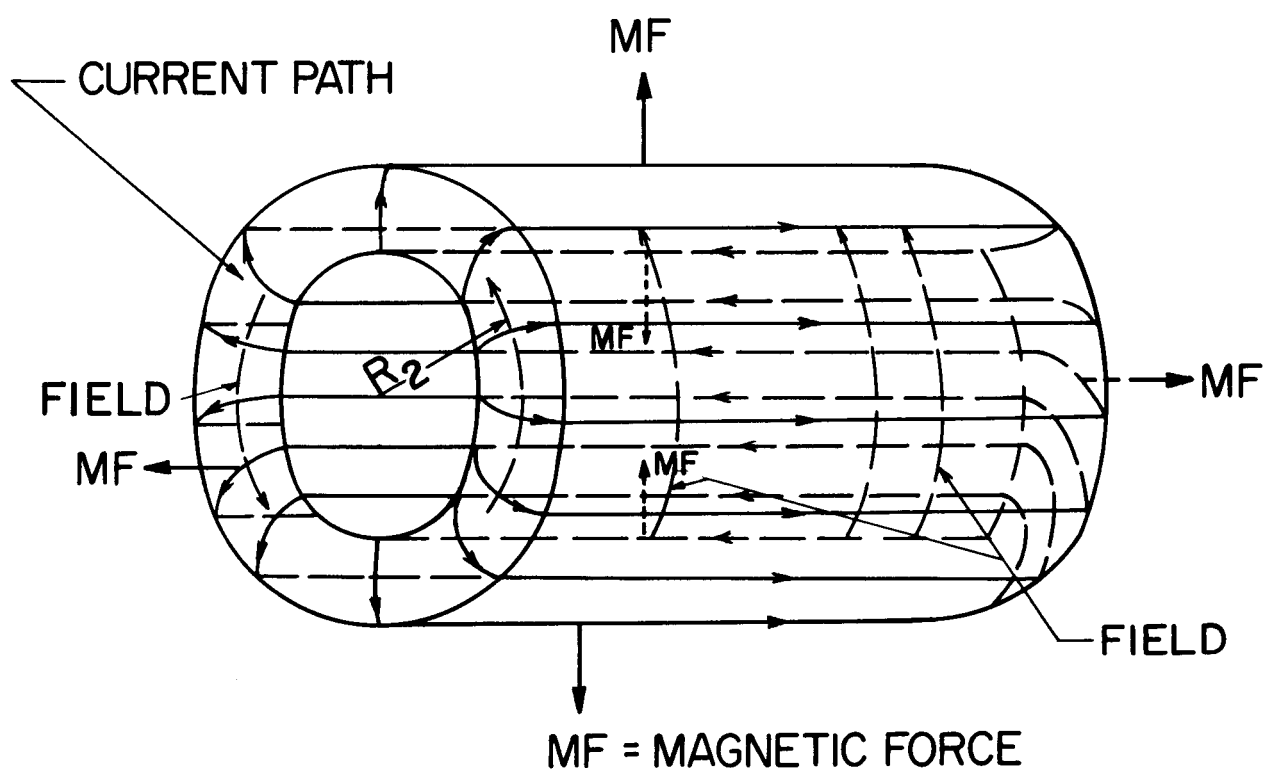


Figure 3. Confined Magnetic Field

in which E_p is the energy of the particle in ergs.

The trajectory of the particle in the field is shown in Figure 4 a for several angles of incidence. The magnetic field is symmetrical about the z axis and follows the torus of which one quadrant is shown as ABCDEFGHA. Note that the depth of penetration towards the z axis is equal to R_2 in the case of particles parallel to the x or y axis but that the depth of penetration is equal to $2 R_2$ if the trajectory is parallel to the z axis. For any angle of incidence in a plane containing the z axis the depth of penetration has a maximum of $2 R_2$.

The coils making up the helical coil will act as passive shields because the windings are designed to completely cover the torus. Actually a layer of copper will be required as insulation for the superconducting coils but its stopping power is the same as that of the superconductor. The equivalent thickness in grams/cm² of the coils and thermal insulation is the density of the material times its thickness in cm with a value of 0.04 taken for the thickness of the insulation. Therefore, the equivalent stopping distance is

$$E = 8.9 (T + 0.04) (\sec \alpha_0 + \sec \alpha_E) \quad (21)$$

The depth of the confined field is

$$X_d = R_2 (\sin \alpha_0 + \sin \alpha_E) \quad (22)$$

The particles as shown in Figure 4b are slowed down in the outer layer, turned around in the magnetic field, and then (if they strike the inner layer at all) they are brought to rest at point P. Of course, many of the particles will not strike the inner wall at all because of the angle of incidence as shown in Figure 4a.

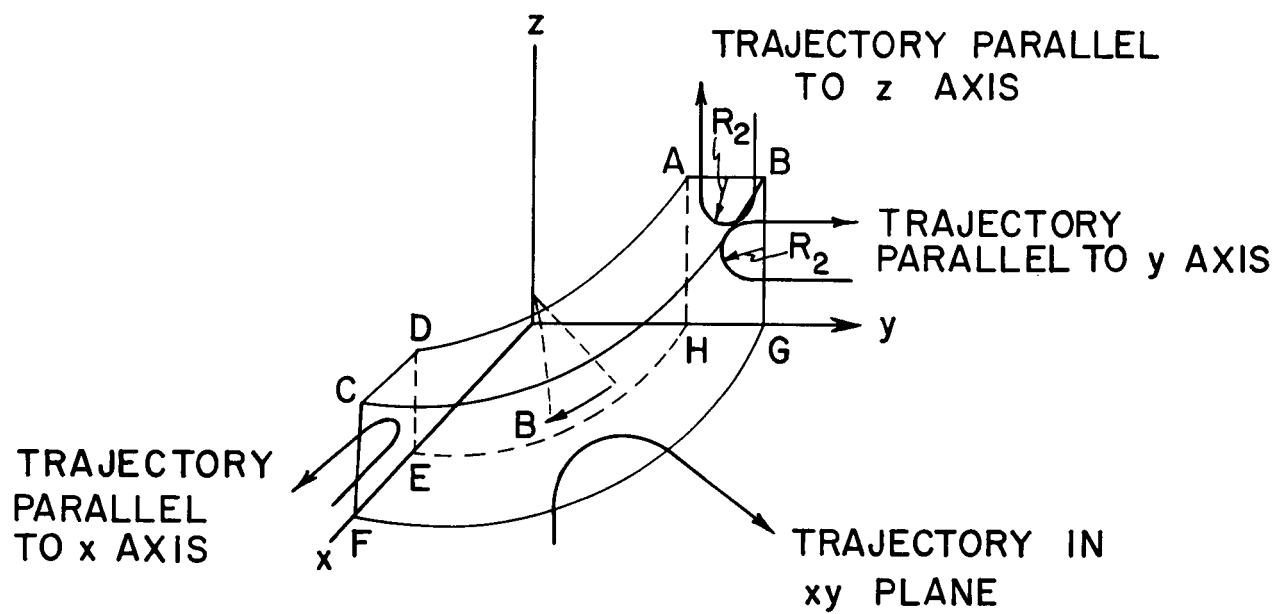


Figure 4a. Trajectory of Particles in a Magnetic Field

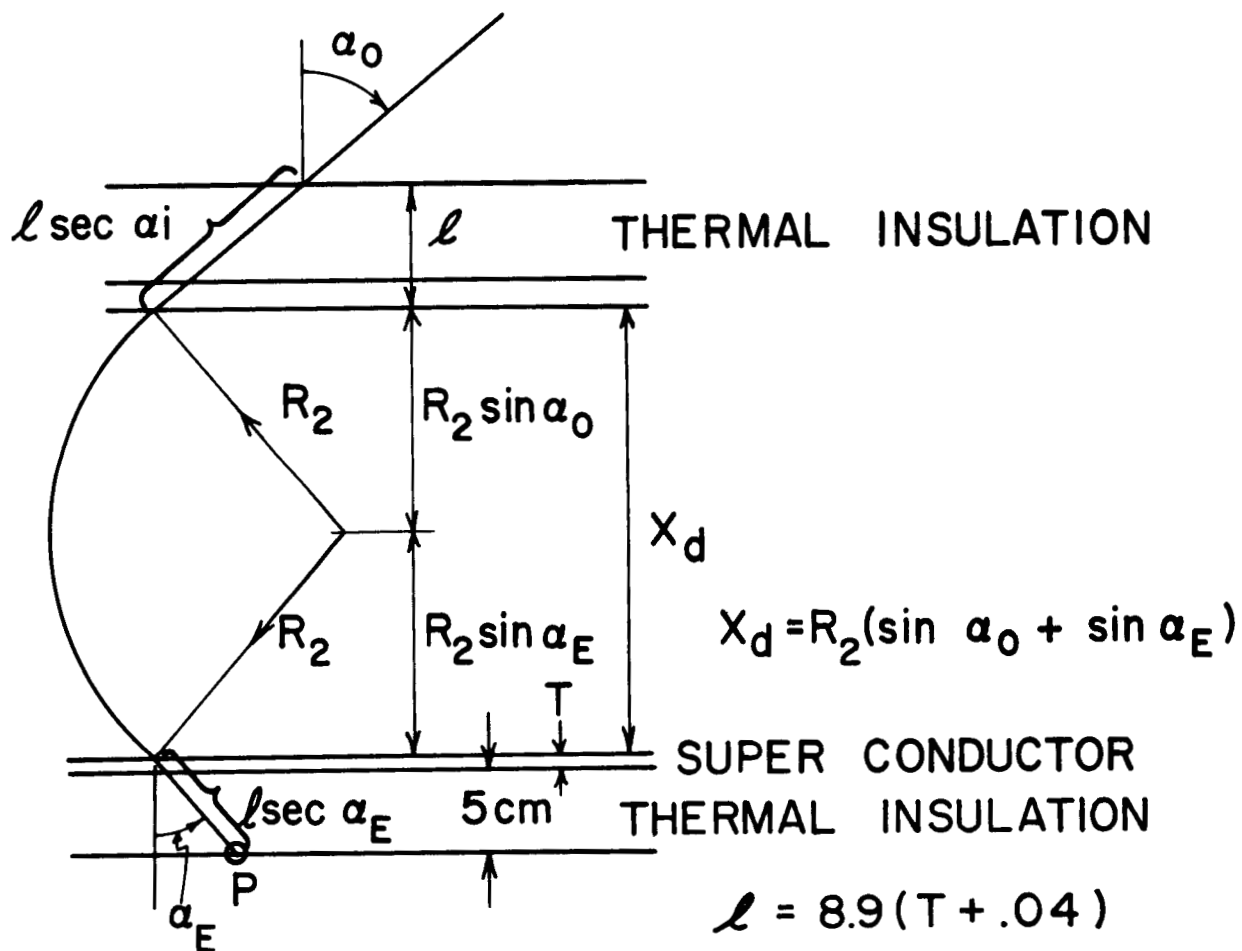


Figure 4b. Dimensions for Determining the Depth of the Confined Magnetic Field

There will be an optimum angle for which the particles will either not reach point P (α_i less than α_o) or will be absorbed in the outer layer so that their energy in the field is low and ν will be small (α_i greater than α_o). To obtain that angle, equations (20), (21) and (22) are combined with the equation for energy loss during passage through matter

$$E_p = E_o \left(1 - \frac{8.9(T+0.04) \sec \alpha_i}{E} \right)^{1/(1+\beta)} \quad (23)$$

in which β is 0.70 by experiment. The final equation for calculating X_d is

$$X_d = \frac{3.86 \times 10^{-2}}{\sqrt{T}} \sqrt{y^2 \frac{E_o^2}{E^2} + 1.86 \times 10^3 y \frac{E_o}{E}} \left[\sqrt{1 - \cos^2 \alpha_o} + \sqrt{1 - \frac{8.9^2(T+0.04)^2}{y^2}} \right] \quad (24)$$

in which

$$y = E - 8.9(T+0.04) \sec \alpha_o \quad (25)$$

and E_o is the energy of the incoming particle in MEV. The values of X_d were found by programming the IBM 1620 computer to seek the minimum X_d by varying α_o by appropriately diminished steps.

D. Magnetic Field in the Crew Space

The confined field is constructed to have no field produced by the coil currents anywhere except in the proper region. For the unconfined field one is faced with the problem of how large is the field in any particular place. For an unconfined field produced by a single turn shaped in the form of a hollow

doughnut the calculations involve elliptic functions. Figure 5 shows the configuration and attendant nomenclature.

General methods for determining the field do not lead to a unique answer so that one resorts to Ampere's law for the magnetic field, H .

$$\bar{H} = \frac{1}{10} \int \frac{\bar{J} \times \hat{r}}{r^2} dv \quad (26)$$

where \bar{J} is the current density vector, \hat{r} is the unit vector directed from the current element toward the point of observation, r is that distance, and dv is the volume element of the current. Equation (27) is the expression for the field at the point b , using the distance constants R_3 and a' . The integral is taken over the angle variables θ' and ϕ' . All of these symbols are shown on Figure 1.

$$\begin{aligned} \bar{H}(b, \beta') = & \frac{Ja'T}{10} \int_0^{2\pi} \int_0^{2\pi} \frac{1}{(R_3 + a' \cos \phi')} \left\{ \left[\hat{i} \cos \theta' (b \sin \beta' - a' \sin \phi') \right. \right. \\ & + \hat{j} \sin \theta' (b \sin \beta' - a' \sin \phi') \\ & - \hat{k} (R_3 \cos \theta' + b \cos \beta' \cos \theta' - R_3 - a' \cos \phi') \Big] / \left[(1 - \cos \theta') (2R_3^2 \right. \\ & + 2R_3 b \cos \beta' + 2R_3 a' \cos \phi') + b^2 + a'^2 - 2ab \sin \beta' \sin \phi' \\ & \left. \left. - 2ab \cos \beta' \cos \phi' \cos \theta' \right]^{3/2} \right\} d\theta' d\phi' \quad (27) \end{aligned}$$

T is the superconducting torus thickness and \hat{i} , \hat{j} , and \hat{k} form the vector triad.

Since we have not found a closed form solution to this equation, we have introduced the approximation $R \cong 10a$. The field on the axis of the torus and at the origin is evaluated by setting $b = R_3$ and

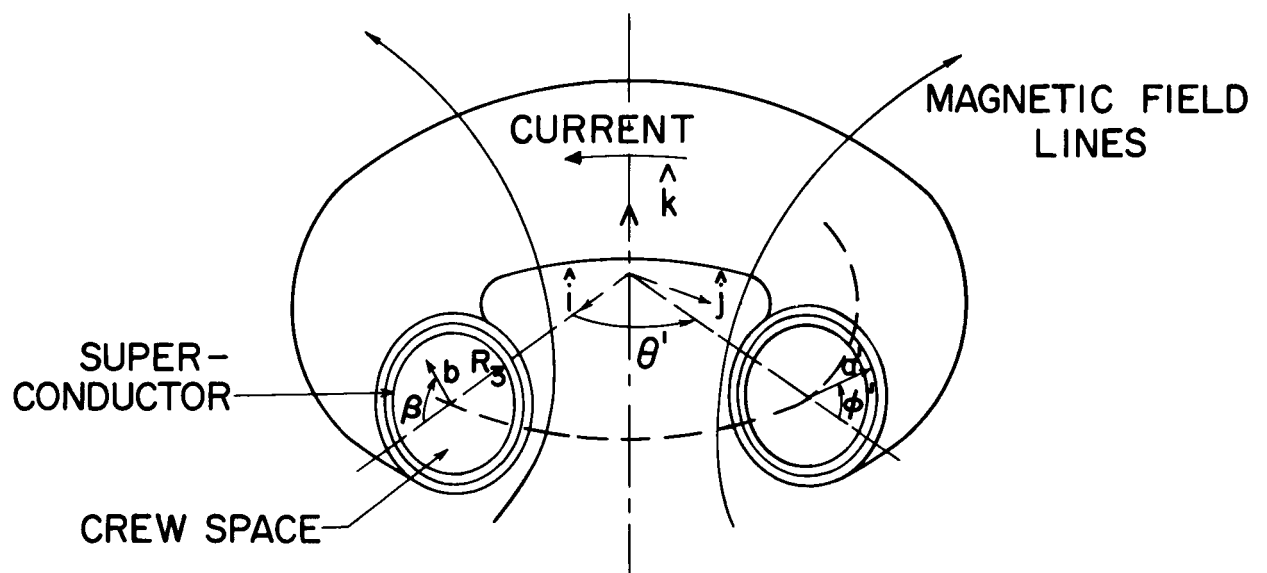


Figure 5. Sketch of Single Turn Coil Radiation Shield

$\beta' = \pi$. The field within the crewspace at its central part is obtained by setting $b = 0$. For the first case, the field reduces to that of a single turn coil

$$\bar{H} = \frac{2\pi I}{10 R_3} \hat{k} \quad (28)$$

in which I is the total current in the superconductor. For the second case, the integral has been evaluated by Simpson's rule and found to be

$$\bar{H} \cong \frac{2 I R_3^2}{10 (a')^3} (0.0017) \hat{k} \quad (29)$$

The ratio of the second to the first field is $0.0017 R_3^3 / a'^3 \pi$. If R_3 / a' is ten as required for the initial assumption, the field within the solenoid is 0.6 times that at the axis of symmetry of the toroid.

III. Vehicle Considerations

This study had a dual purpose: the basic concepts were examined for practical aspects, and secondly, the concepts were applied to sizes of spacecraft that are practical so that an optimization process might be carried out. Thus, some basic assumptions were made at the start from which various spacecraft configurations were postulated, various structures were hypothesized, and various superconductor parameters were chosen.

A. Basic Assumptions

As indicated in the Introduction there are three sources of ionizing radiation: galactic cosmic rays, solar cosmic rays, and geomagnetically trapped radiation. Galactic cosmic rays are made up of protons, α particles, and heavier ions. The heavy ions are relatively easy to stop with small thicknesses of passive shields. However the majority of protons have energies greater than one GeV which are not easy to stop with any shield. Solar cosmic rays are protons with most of them having smaller energies. Since a small passive shield (one or two grams/cm²) will stop protons of less than 30 MeV, the important range of protons is 30 MeV to one GeV. Van Allen radiation contains protons in high fluxes on the order of several hundred MeV. There are also high fluxes of electrons in the order of 40-1000 keV; however, with the small mass of electrons the radius of curvature according to equation (20) in a magnetic field will always be smaller than that of protons for a comparable energy. At 100 MeV the ratio of electron

to proton trajectory radius of curvature is 0.23 and at 1000 MeV the ratio is 0.59. Thus, any magnetic field safe for protons is safe for electrons. (Of course, the electrons turn in an opposite sense from protons which may complicate the leakage problems around hatches to be discussed later.)

The above data indicate that a representative range of energy for the incident particles would be between 100 and 1000 MeV, say 100, 200, 500 and 1000 MeV. Shielding for electrons will not be considered in detail in this report.

The spacecraft must be large enough to hold a man and yet not too large to be lofted with a booster in the foreseeable future. We have chosen 10, 100, 1000, and 10,000 cu. ft. as reasonable volumes to be shielded.

As stated above, superconducting coils will be needed. The best found to date is Nb_3Sn with NbZr being commercially produced but not as good. The properties of these two are given in Table I.

Table I

Properties of Superconductors

| Property | Nb_3Sn | $\text{Nb } 25\% \text{ Zr}$ |
|---------------------------------------|------------------------|--|
| Critical Temperature ⁽¹⁴⁾ | 18°K | 10.8°K |
| Critical Field ⁽¹⁵⁾ | 180 K gauss | 77 K gauss |
| BJ Relation ^(15, 21) | 6×10^9 | $8 \times 10^8 \frac{\text{gauss amperes}}{\text{cm}^2}$ |
| Annealing Temperature ⁽²⁰⁾ | 1000°C | ---- |
| Training Effect ^(17, 18) | ---- | Present |
| Coil vs. Single Wire ⁽¹⁷⁾ | ---- | Large effect |
| Cost (1963) | \$1300/lb. | \$400/lb. |
| Density | 8.8 gr/cc | 8.0 gr/cc |

Note: The training effect refers to the decrease in critical current or increase in critical field that occurs in coils of superconductors for sequential starts and stops of the current.

Thermal insulation is needed because of the cryogenic temperatures required. Liquid helium will be mandatory. One notes that the values of critical currents and fields fall off rapidly before the critical temperatures are reached in hard superconductors such as Nb_3Sn and NbZr .⁽¹⁵⁾ The best insulators have thermal conductivities on the order of 10^{-4} cal/cm°C sec and densities on the order of 0.075 gm/cc.

Since the confined field will completely surround the spacecraft, a hatch will be needed at least large enough for a man to pass through. To be specific the diameter will be set at 50 cm.

B. Spacecraft Configurations

Figure 3 shows a cylindrical configuration, and indeed this was chosen as the first to study. Various ratios of length to radius were chosen (8/1, 4/1, 2/1, 1/1 and 1/2) to cover the range and to show whether an optimum ratio existed. Figure 6 indicates the trajectories of protons passing through a confined field around a cylindrical crewspace. One notes the curvature in the different halves; in fact, at the joint on the right hand side the proton executes an "S" turn directly into the crewspace. Thus, a passive shield is required to stop those protons. It is almost self-evident that one cannot add a second confined field because there will always be a joint of oppositely directed fields.

Figure 7 shows a preliminary sketch of a spacecraft with a spherical crewspace, with the confined magnetic field surrounding the crewspace, and with the passive shield at the hatch on the left. One notes the protuberance on the right-hand side added to prevent axial particles from penetrating the thermal insulation.

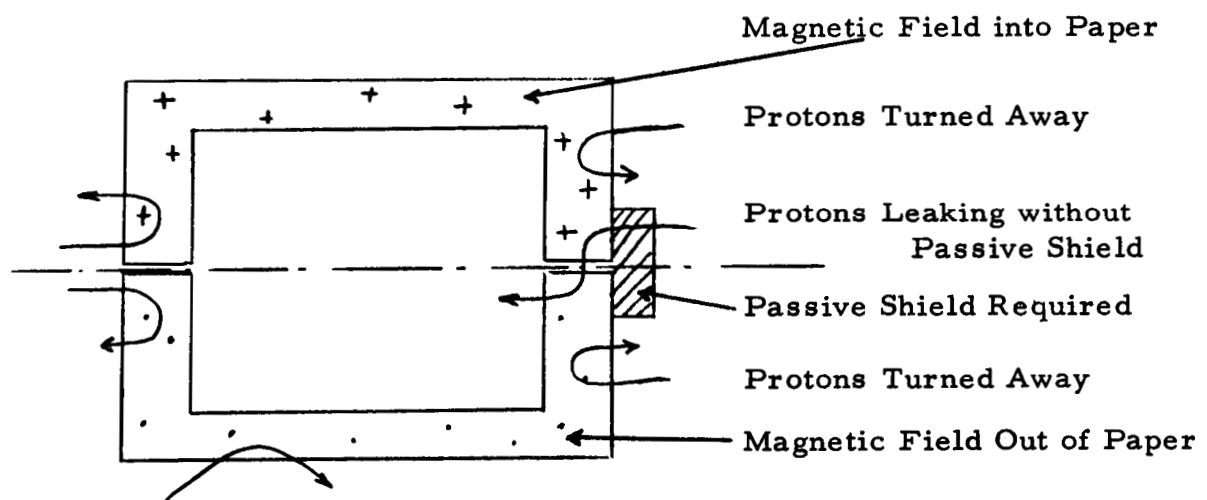


Figure 6. Principle of Proton Leaks

PRELIMINARY

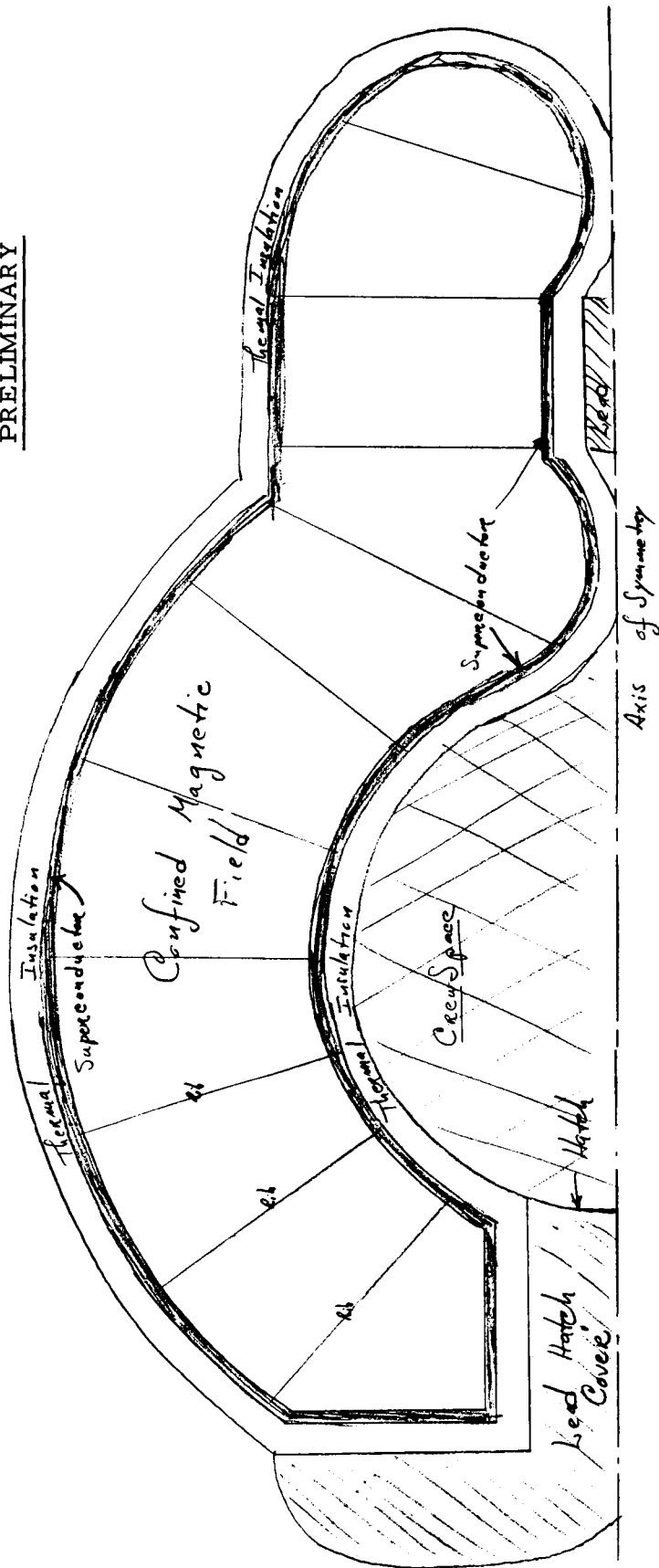


Figure 7. Preliminary Sketch of Magnetic Shielding Configuration for a Sphere

Figure 7 shows cross ribs required to support the magnetic pressures on the coils. This configuration has been corrected as shown on page 50.

Figure 8a shows the construction of the toroidal spacecraft. The crewspace is surrounded by a double helical coil. The confined field is maintained between these windings. To provide access to the crewspace a shielded hatch may be added. There are two radii whose ratio is to be varied: the radius of the crewspace cross section and the distance of the cross section from the axis of the torus. For the given volumes we chose four ratios, $1/2$, $1/4$, $1/8$, and $1/16$. Figure 8b shows that if the field space would meet at the axis of the torus a passive shield would be needed to prevent "leaks". Therefore, the computer was set to drop out all cases in which the field space met at the center. Because there are no "leaks" in the open center shape requiring a passive shield, weights were calculated for toruses with and without a passive shielded hatch.

With the trend toward spaceships which can be assembled in space, we have calculated the weights of spacecraft made up of strings of spherical modules. Each module is designed to be independently protected from particles. Each is a sphere with one or two hatches. Figure 13, page 51, shows the construction: One end of the string will correspond to the left hand end of the cylinder on Figure 6 and be called a blind end. Center modules will have two openings so that it may be joined to two other modules. The hatch end will have one opening for connection with the string and a passively shielded hatch for entrance to the whole string after construction. Besides the obvious advantage of construction in space, the weight of the hatch is spread out over a larger volume so that the overall weight decreases.

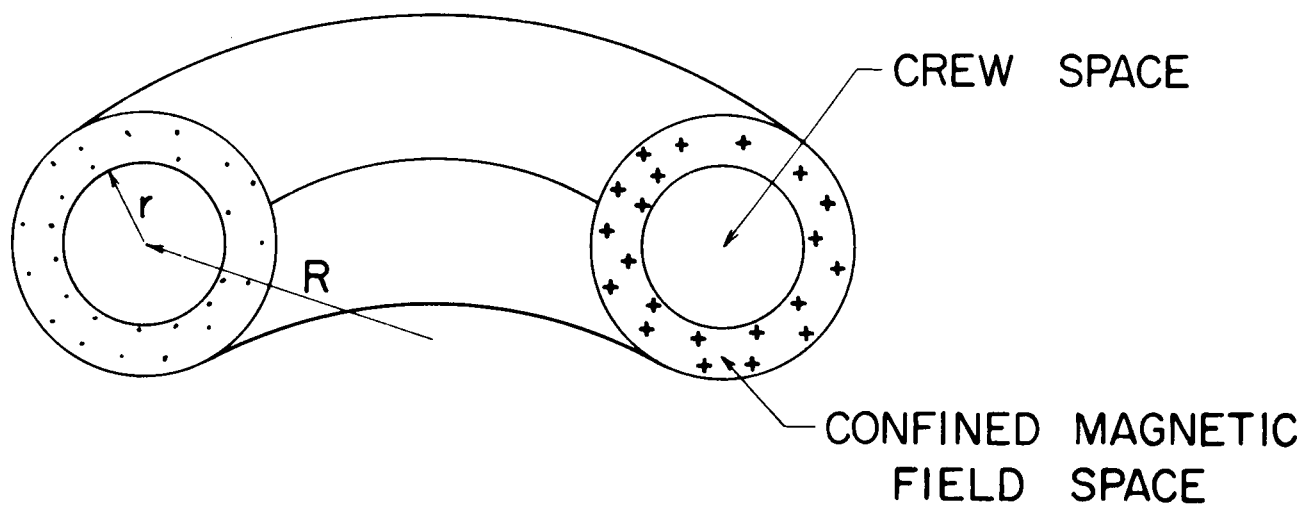


Figure 8a. Torus Cross Section

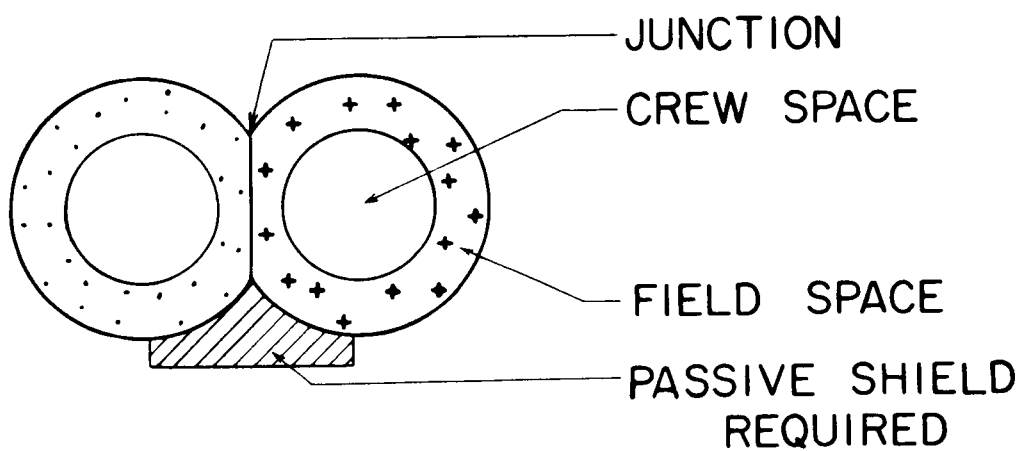


Figure 8b. Junction of Magnetic Field Spaces

C. Hatch Construction

The diameter of the hatch was set at 50 cm to permit passage of a man. For the different energy protons various materials and minimum thicknesses were used to keep the volume small. Table II shows the data. A basic design was made

Table II
Passive Shield Materials for the Hatch

| Proton Energy MEV | Material | Thickness cm | Density grams/cm ³ |
|----------------------|--------------|-----------------|----------------------------------|
| 100 | polyethylene | 7.7 | 0.92 |
| 200 | polyethylene | 26.1 | 0.92 |
| 500 | aluminum | 54.8 | 2.70 |
| 1000 | lead | 54.4 | 11.3 |

up for the spherical shape and used on the toroidal and modular configurations with only slight modifications. In the calculations the weight of the hatch was computed separately so that its part of the total might be determined.

For the toroidal shape a passive shield is not needed because the oppositely directed fields do not have an interface. Mechanical doors might be used just as in any ordinary hatch except that joints in the windings or special configurations would be required. If joining techniques are developed, mechanical hatches will be designed as a matter of course. It might

be possible to make the torus from segments each of which is independently constructed. Each would have its own coils and its own cooling system. Entrance could be obtained by removing one segment although the field should be cut off as it would no longer be confined.

There is another possibility for protecting the hatch on the cylindrical and spherical shapes. Unconfined magnetic fields have forbidden zones one of which could be placed at the hatch. Thus, a small unconfined field source could be used for a small area in place of a large one for the whole spacecraft. Since it would be small, it would not interfere with the confined field used as the major protector. Being small the source could be removed or even shut off during use of the hatch. This plan was not pursued completely because of lack of time in this contract.

D. Structural Requirements

Just as there are forces on the ionized particles there are forces on the current carrying conductors. This force depends upon the magnetic field, the current, the length of the conductor, and the angle between the current and fields. For 1000 Mev protons the force per unit of conductor is

$$F/L = BI = BJT^2 = 4000 \text{ lbs/in.} \quad (30)$$

With windings directly touching this force is equivalent to a pressure 4000 psi which can not be supported by the wires alone.

The derivation for the weight of struts has been given in general by Levy⁽¹¹⁾ but for the cylindrical model we propose the following simplified derivation.

Given a cylindrical torus such as shown on Figure 3 that has a length L and radii r_o and r_i . The area on the end is thus

$$\pi(r_o^2 - r_i^2) = A_t \quad (31)$$

and since the magnetic pressure is $B^2/8\pi$, the force on the end becomes

$$F_t = \frac{B^2}{8\pi} (r_o^2 - r_i^2) \pi \quad (32)$$

This force must be supported by N_s struts of area A_s , density ρ_s , length L , and carrying a stress σ_s .

$$F_t = N_s \sigma_s A_s \quad (33)$$

The weight of these struts will be

$$w_s = N_s A_s L \rho_s \quad (34)$$

These may be combined to obtain

$$w_s = \frac{B^2 \pi (r_o^2 - r_i^2) L \rho_s}{8 \pi \sigma_s} \quad (35)$$

from which using equation (18) and noting that the expression $\pi(r_o^2 - r_i^2)L$ is the volume of the flux

$$w_s = V_f T \left(\frac{6 \times 10^9 A}{20 \sigma_s} \right) \quad (36)$$

For many materials ρ_s/σ_s is approximately 10^{-6} in^{-1} ($4 \times 10^{-10} \text{ cm grams wt/dyne}$). Equation (36) becomes

$$w_s = 0.12 V_f T \quad (37)$$

where w_s is expressed in grams weight.

Although this equation was derived for struts it would be equally as good for any cross section of support. With this in mind, the struts could be converted to plates of the same cross sectional area. By using Tresca's failure criterion, the value of the limiting stress is not changed by adding a stress of the same sign perpendicular to the original stress. (In this simplified derivation corner effects are neglected.) Thus, the weight of a plate can be calculated with equation (37) that will support the whole coil.

E. Magnetic Field Engineering

Magnetic fields should be as high as possible to keep the size down. With large fields the energy density increases so that the energy stored in the field will be large and the currents large to produce the fields. The only way to economically (in terms of power dissipated, heat dissipated, or weight of coils) use the electromagnetic fields is to employ superconducting materials. These raise four problems: availability, refrigeration, energization, and structural possibilities.

At the present time the commercially produced and sold superconductor is niobium zirconium. This wire is supplied in 5, 10 and 15 mil diameters in lengths up to 20,000 ft. There are several grades which include alloys of 25, 33, and 50% **Zr**. Joints are made by soldering but a high resistance is thereby added. The wire may be coated with nylon, formvar, or copper as an insulation. When tested in single turns, the critical field at 4.2°K is 60-80 kilogauss depending upon the grade. When tested in a coil form, the critical field increases with cycling. Thus, the critical magnetic field of the coil may start at 40 kilogauss and be raised to 50 kilogauss by cycling.

Niobium tin is a much better superconductor in that it has a higher critical temperature and a higher critical field. At 4.2°K the critical field is about 180 kilogauss. However, coils do not produce such high fields. Martin⁽¹⁶⁾ et. al. reports construction and test of a small coil that produced a field of 101,000 gauss in a liquid helium bath.

Nb₃Sn is constructed by enclosing a tin rich mixture of niobium tin in a hollow niobium tube. This composite wire is sealed and reduced mechanically to wires about 0.038 cm in diameter.⁽²²⁾ In this state the wire is flexible enough to wind coils. The assembly is then heat treated by soaking at 1000°C periods up to 24 hours. Since there is a size effect, these coils have been constructed mainly by trial and error. It is expected that with further testing the techniques can be standardized to become commercial. There is no training effect in coils made from Nb₃Sn compound.

Other materials have been found to be superconductors, but they are formed from even more exotic elements. Vanadium, Gallium, Thorium, Tantalum, Indium, Rhenium, Tellurium, and compounds thereof have all been tested. Most of these have critical temperatures (2-4°K) and are not in good supply commercially.

Refrigeration is taken for granted with these materials. Cryogenic apparatus have low efficiencies and are not usually of a closed circuit type. A small refrigerator is described by Hoffman⁽²³⁾ for cooling a maser to 4°K. The apparatus shown in the photographs is about six feet long by one foot in diameter which indicates the required volume to cool a laser of one cubic inch volume. An expansion cycle employing regenerators coupled with a

Joule-Thomson circuit constitutes the process. The paper tells how the reliability of the components is provided by care in construction and redundancy in parts. Extreme care is exercised in preventing contamination of the coolants. These portable closed-cycle systems are available commercially that could be adapted as a part of the protective system. Since the efficiency is about 5%, a 500 k watt power supply would be needed for a 1000 cu. ft. spacecraft on earth. In space the power required will be smaller because the ambient temperature is low. Radiant heating from the nearby earth and sun (if the spacecraft is in an orbit about the earth) can be minimized by properly coating the outside surface.

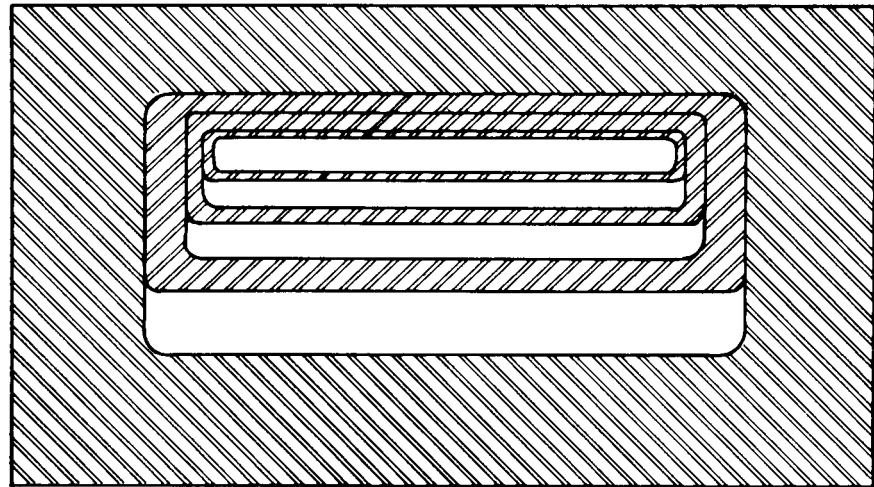
The energy contained in the field will be large. With an energy density of $B^2/8\pi$ and a flux volume of 2 megaliters for a 1000 cu. ft. spacecraft the energy could be as high as 10 megajoules. The coil could be charged in one day using a 1000 volt DC supply. The discharge is the source of worry. If the coil were to go "normal," the heat generated (roughly 25,000 cal/gram) would quickly melt down the coil, most of the supports, and some of the spacecraft. Two features may be suggested as possibilities for decreasing the danger. Damper windings made of copper may be added to absorb and redistribute the magnetic field energy. This has been suggested by Minuich⁽²⁴⁾ with details worked out. The coil could be constructed of independent segments which would allow the energy from one coil to be picked up by the others in the magnetic circuit. This implies, of course, that operation is not occurring near the critical points for any of the segments; otherwise the redistribution

of energy would be exponentially self destroying.

The structure of the coils must include two provisions: an adequately strong supporting structure and a means for maintaining a constant field. The strength of structure required is described in section III D above. This is given as a tension plate and with a three dimensional coil the concept leads to a solid support for the coil. Obviously, this is impossible. Single plates in rows must be used with back up structure behind the coils, since the wires must be supported at points no farther than 0.25 cm apart at the indicated pressures. These plates will add to the overall weight of the supporting structure which has not been included in the calculation presented later.

In the coils shown in Figure 3 the field is not constant but varies with the radius. The coils might be altered as shown in Figure 9 to add turns as the radius increases. The number of ampere turns is larger at the outer edge than it is at the inner edge. By apportioning the coils the variation in field strength may be held as low as desired. The construction eliminates the spaces that would occur in the outer row of coils since the outer circumference is larger than the inner one.

With the above consideration and dimensions for the several spacecraft, calculations have been made which are reported below.



AXIS OF SYMMETRY

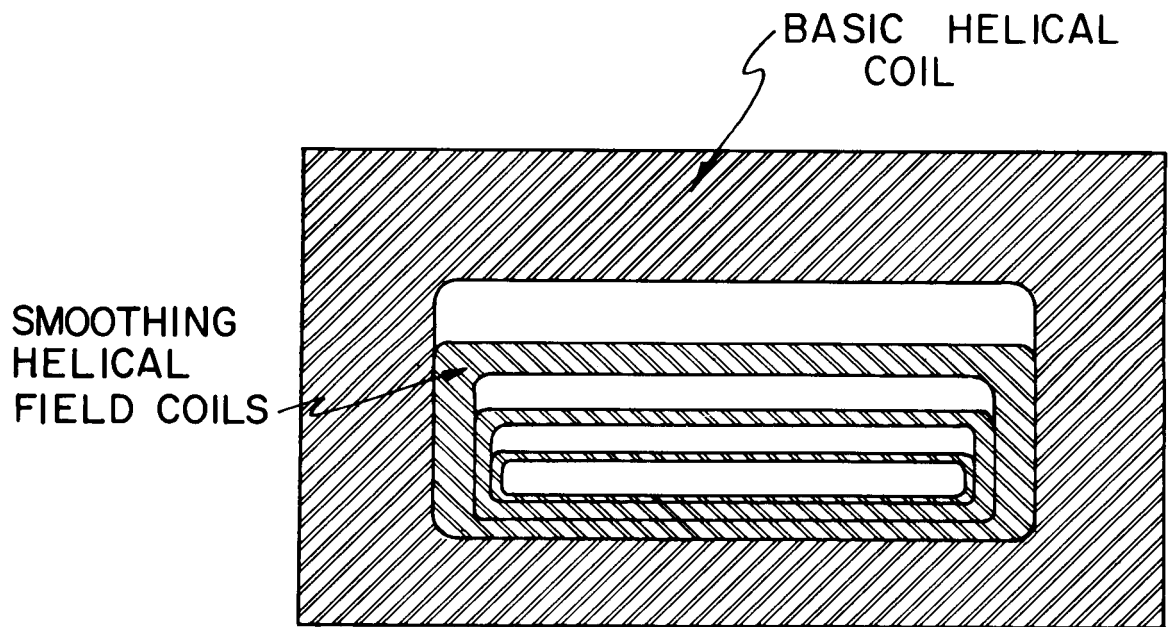


Figure 9. Field Smoothing Coils to Alleviate Radial Variation

IV. OPTIMIZATION PROCEDURES

A. Possible Criteria

There is always a basic mission for which any spacecraft is designed from which the specifications are promulgated. But underlying the whole proceedings are the size, weight, and cost limitations. The first two because of considerations external to the spacecraft and the last because of economics. This study of shielding requirement and possibilities was placed under the limiting category of weight because the size is still unimportant and the cost is of small consequence in a conceptual study. Thus, the weights of the various parts of the radiation shield were calculated and compared to show the possibility of minimizing the weight.

Optimization was achieved in this work by reducing the size, by computing the optimum wire size, and by choosing the lowest weight from a series of calculations. First, the size of the confined field space was minimized by including the absorption of incident protons by the superconducting windings. (The protons enter the space at a reduced energy and velocity; hence, by equation (3) the radius of curvature of the trajectory and the space size were reduced.) Second, the angle of incidence was computed for protons of different energies which optimized the depth of the field space for each superconducting wire diameter. And third, radiation shield weights were calculated for many thicknesses of superconductor and the minimum weights taken from those data.

As shown above in Section III, the proton absorption was taken to be virtually the same as that for copper. Data for copper was taken from the

paper by Sternheimer.²⁵ The insulation was assumed to be 4% as good an absorber (weight-wise) as copper.

The values for α_o , proton angle of incidence as defined in equation (24), were calculated for 100, 200, 500, and 1000 MeV protons and for superconductor coil wire diameters of 1.563×10^{-3} to 12.8 cm. For each value of these two parameters, the thickness of magnetic field is shown in Table III. The general size was kept between 1500 and 20 cm to obtain minima in the weight calculations. Table III shows that the field space must be larger for more energetic protons and at large wire diameters the field size is decreased considerably. However, the minimum weights were found to lie in the same band of X_d values for all spacecraft configurations. These values are boxed in Table III. Furthermore, one notes that these values are near 180 cm for all proton energies. The weight penalty occurs because larger superconducting wire cross section are required for the more energetic protons.

Total weights were calculated for the shield so that a minimum could be determined. Figure 10 shows a logarithmic plot of the results for a spherically shaped spacecraft. There is a definite minimum shown in each case. Note that the weights were larger for more energetic protons, and that the weights are large, ranging from six to one hundred metric tons.

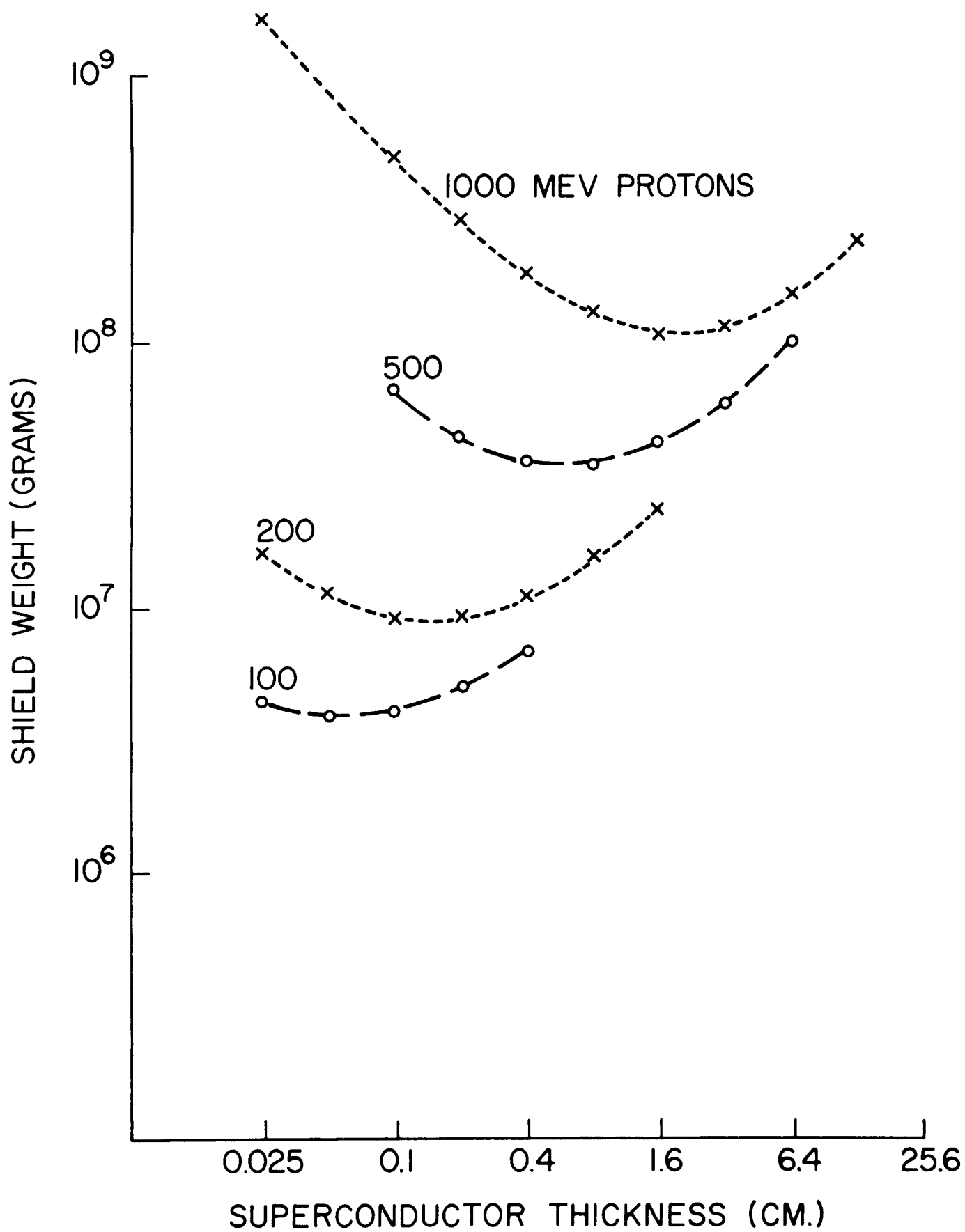


Figure 10. Spherical Shape Weight Optimization

Table III

Magnetic Field Depths, X_d in cm

| Proton Energy in MeV | 100 | 200 | 500 | 1000 |
|----------------------|-------|--------|--------|--------|
| Wire Thickness | | | | |
| .0015625 cm | 806.* | 1,205. | 2,137. | |
| .0031250 | 568. | 851. | 1,512. | |
| .006250 | 400. | 600. | 1,070. | 1,656. |
| .01250 | 285. | 422. | 740. | 1,171. |
| .0250 | 199. | 302. | 522. | 829. |
| .050 | 136. | 211. | 367. | 588. |
| .100 | 93. | 145. | 257. | 407. |
| .200 | 59. | 101. | 177. | 285. |
| .400 | 32. | 68. | 125. | 198. |
| .800 | | 43. | 86. | 139. |
| 1.600 | | 21. | 58. | 95. |
| 3.200 | | | 36. | 64. |
| 6.400 | | | 19. | 43. |
| 12.800 | | | | 25. |

* Note: All figures are carried to eight figures on the IBM 1620 computer.

B. Weight Calculations

1. Cylindrical Shape

The first calculations were made on cylindrical shapes. According to the schemes given above, the weights were found for ratios of radius to length of the cylinders from 1/8 to 2. Table IV shows the weights. The values increase as both the energy of incident protons and the volume of spacecraft are increased. This was expected.

Table IV
RADIATION SHIELD WEIGHTS
CYLINDRICAL SHAPE

| Volume | r/l | Proton Energy | 100 | 200 | 500 | 1000 MEV |
|---------|-------|---------------|-------------|------|-------|----------|
| | | | Metric Tons | | | |
| 10 | 1/8 | | — | — | — | — |
| cu. ft. | 1/4 | | .6 | 1.4 | 4.2 | 10.9 |
| | 1/2 | | .6 | 1.5 | 4.6 | 12.1 |
| | 1 | | .6 | 1.7 | 5.4 | 13.8 |
| | 2/1 | | .7 | 2.0 | 6.6 | 16.4 |
| 100 | 1/8 | | 1.6 | 3.2 | 8.4 | 20.0 |
| cu. ft. | 1/4 | | 1.5 | 3.3 | 9.2 | 21.6 |
| | 1/2 | | 1.6 | 3.7 | 11.1 | 25.5 |
| | 1 | | 1.6 | 4.4 | 14.4 | 32.4 |
| | 2/1 | | 2.0 | 5.5 | 19.1 | 43.5 |
| 1000 | 1/8 | | 4.1 | 8.7 | 24.1 | 51.1 |
| cu. ft. | 1/4 | | 4.2 | 9.5 | 28.2 | 60.5 |
| | 1/2 | | 4.3 | 12.0 | 36.3 | 78.9 |
| | 1 | | 5.0 | 13.7 | 48.7 | 108.2 |
| | 2/1 | | 6.3 | 18.5 | 68.2 | 158.7 |
| 10,000 | 1/8 | | 12.0 | 27.0 | 83.5 | 173.5 |
| cu. ft. | 1/4 | | 12.5 | 30.5 | 103.5 | 222.0 |
| | 1/2 | | 14.4 | 37.5 | 136.5 | 304.0 |
| | 1 | | 18.0 | 49.0 | 189.0 | 439.0 |
| | 2/1 | | 23.0 | 68.0 | 272.0 | 663.0 |

To compare various types of shields and various configurations these data were converted to standard dimensions. The shield weights were divided by the volume of the shielded crewspace. The "Loading Index" derived by Dow⁸ was used as the other parameter. It is the ratio of the range of protons in the shield to a characteristics length of the shield. The index is expressed as

$$L.I. = \frac{CE^{1.75}}{r} \quad (38)$$

in which C is 1.1×10^{-3} grams/cm² MeV^{1.75}, E is the proton energy in MeV and r is a characteristics length in cm. For a passive shield an obvious choice for r would be the shield thickness in which case the Loading Index would be close to one. This would be useful in comparing the weights of different passive shielding materials. However, this dimension is non-existent in an active shield. Actually, the dimension should be present in both types of shields such as a factor of the shielded volume. Therefore, to make the Loading Index dimensionless, the radius of the equivalent volume sphere was chosen. Figure 11 shows the data plotted for comparison with other configurations and with a polyethylene shield.

To illustrate the use of these graphs we examine the line AB drawn on Figure 11 at a Loading Index of 0.13. This value occurs for two combinations of proton energy and volume: (1) 200 MeV and 100 cuft. volume (radius r being 88 cm), and (2) 500 MeV and 10,000 cuft. volume (radius r being 189 cm). The curve for the polyethylene shield reaches 0.7 grams/cc at this index. For case (1) the weight would be 2.0 metric tons and 200 metric tons for case (2). The curves for active shields indicate 1.3 grams/cc or 3.6 metric tons for case (1), and 0.35 grams/cc or 99 metric tons for case (2). Thus, the

passive shield is lighter for low energy protons but heavier for high energy protons. In general then, the lower the curve is on the graph, the lighter the radiation shield is for any given shielded volume.

2. Spherical Shape

Calculations were made on a spacecraft having a spherical shape. Figure 7 shows the configuration used for the first weight calculations made for a spherically shaped crewspace. It was suspected that some parts of the radiation system might be heavier than the others so the computer was programmed to print out more subsidiary numbers. In particular, the weight of superconducting coils, the insulation, the support structure, the passively shielded hatch, and the total weights were printed out. Table V shows the total weights in kilograms for the standard volumes and proton energies. The weights were broken into the four parts by percentages.

Again the weights are large and the percentage devoted to the hatch is large. Even so, the values are less than those for the cylindrical spacecraft as shown on Figure 11.

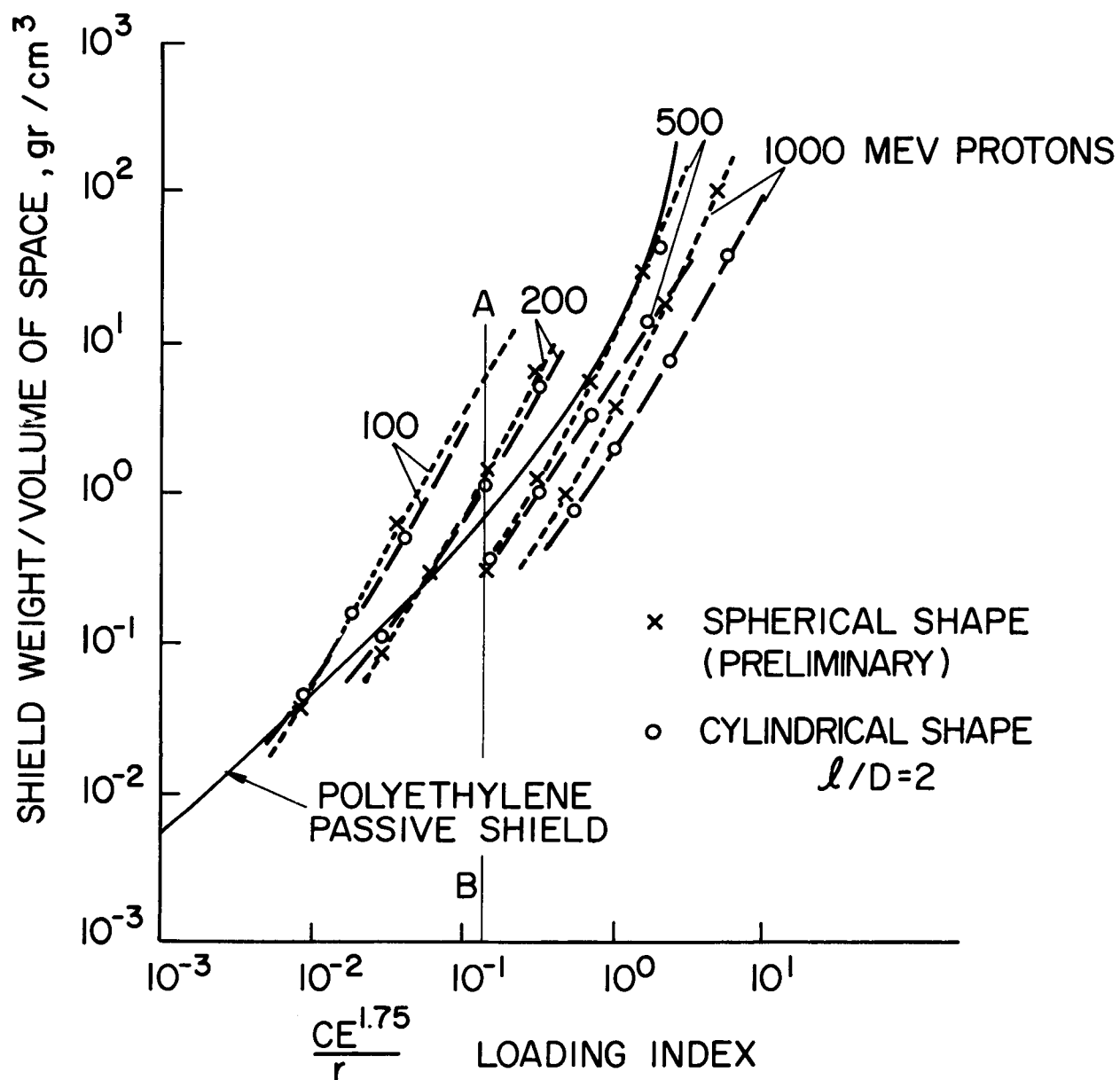


Figure 11. Comparison of Shielding Weights
I - Sphere, Cylinder, Polyethylene

TABLE V

Magnetic Shielding Structure Weights for
Spherical Shaped Spacecraft

| Volume | Proton Energy | | | |
|-------------|---------------|-----------|-----------|------------|
| | 100 MEV | 200 MEV | 500 MEV | 1000 MEV |
| 10 cuft | 613 Kg | 1,813 Kg | 8,045 Kg | 30,656 Kg |
| Hatch | 17.6% | 14.5% | 33.6% | 68.0% |
| Super Cond. | 58.5 | 68.4 | 49.7 | 21.2 |
| Insulation | 6.4 | 1.9 | 0.7 | 0.3 |
| Structure | 17.5 | 15.2 | 16.0 | 10.5 |
| 100 cuft | 1,783 Kg | 3,913 Kg | 15,336 Kg | 49,427 Kg |
| Hatch | 8.4% | 27.4% | 35.3% | 54.8% |
| Super Cond. | 60.8 | 41.7 | 40.5 | 27.8 |
| Insulation | 6.5 | 4.5 | 1.2 | 0.4 |
| Structure | 24.3 | 26.4 | 23.0 | 17.0 |
| 1000 cuft | 4,074 Kg | 9,198 Kg | 34,818 Kg | 108,012 Kg |
| Hatch | 17.5% | 28.3% | 36.6% | 56.3 |
| Super Cond. | 33.7 | 31.4 | 31.3 | 21.2 |
| Insulation | 14.4 | 6.7 | 1.7 | 0.7 |
| Structure | 34.4 | 33.6 | 30.4 | 21.8 |
| 10,000 cuft | 10,539 Kg | 24,386 Kg | 89,272 Kg | 280,550 Kg |
| Hatch | 28.0% | 27.2% | 56.7 % | 56.3% |
| Super Cond. | 14.8 | 22.5 | 13.4 | 15.5 |
| Insulation | 25.0 | 9.5 | 2.8 | 0.8 |
| Structure | 32.2 | 40.8 | 27.1 | 27.4 |

3. Toroidal Shape

A spacecraft in the shape of a torus has some peculiar advantages: should an artificial gravity be desirable, the bicycle tire (a torus) model has been advanced. The confined field is particularly simple as shown on Figure 8a. There is the possibility of eliminating the passively shielded hatch as discussed in Section III. Construction would be particularly simple. The shape is amenable to construction as a single turn coil or a helical coil. Even force free coils have been proposed for this shape.²⁶ In view of the above advantages we computed weights for the toroidal shape.

Since there are two basic radii involved, the radius from the axis of symmetry to the center of the cross section and the radius of the cross section, ratios were chosen as 2/1, 4/1, 8/1, and 16/1. It immediately became apparent that the ten cubic foot size and that the 16/1 ratio for the 100 cubic foot size were impossible. It was found also that the center hole in the torus could not be filled with a confined field as shown in Figure 8b. This last limitation meant that the weights calculated might not be a minimum because all values of superconducting coil wire size were not available for use.

The minimum weights that we calculated are shown in Table VI as metric tons (1000 Kg.). The percentage figures represent the passively shielded hatch weights. The weights are also shown for the spherically shaped spacecraft for comparison. In most cases they are larger than the spherical except for the large sizes. It is possible that for very large sizes the torus might be lighter.

TABLE VI

Magnetic Shield Structure Weights-Torus Hatch

| Volume in cuft | R/r | Proton Energy in MEV | | | | | | | |
|-------------------|-----|----------------------|------|-------|------|-------|------|--------|------|
| | | 100 | | 200 | | 500 | | 1000 | |
| | | Toroidal | | | | | | | |
| | | Wt | % | Wt | % | Wt | % | Wt | % |
| 100 | 8 | 2.8 | 12.2 | 6.1 | 21.0 | 21.1 | 28.5 | 62.8 | 47.5 |
| | 4 | 2.1 | 17.5 | 5.1 | 14.9 | 16.8 | 37.8 | 52.9 | 37.3 |
| | 2 | 2.1* | 5.2 | 6.8* | 3.9 | 19.4* | 13.9 | - | - ** |
| 1,000 | 16 | 9.1 | 7.6 | 17.7 | 14.3 | 54.7 | 37.4 | 156.9 | 37.3 |
| | 8 | 6.6 | 11.0 | 13.2 | 20.2 | 43.8 | 28.2 | 129.9 | 47.4 |
| | 4 | 4.9 | 15.7 | 10.2 | 27.6 | 35.4 | 37.3 | 106.6 | 36.0 |
| | 2 | 5.4* | 5.2 | 11.4* | 9.5 | 32.1* | 26.9 | 105.1* | 26.0 |
| 10,000 | 16 | 23.8 | 3.2 | 42.7 | 12.9 | 124.5 | 36.1 | 337.8 | 36.5 |
| | 8 | 17.4 | 4.8 | 32.2 | 18.3 | 98.4 | 27.2 | 285.2 | 46.5 |
| | 4 | 13.2 | 10.2 | 25.4 | 25.4 | 81.3 | 36.3 | 246.9 | 35.3 |
| | 2 | 11.3* | 10.2 | 22.2* | 19.0 | 70.8* | 46.2 | 216.9* | 45.8 |
| | | Spherical | | | | | | | |
| 100 | - | 1.8 | 35.3 | 3.9 | 54.8 | 15.3 | 8.4 | 49.4 | 27.4 |
| 1,000 | - | 4.1 | 36.6 | 9.2 | 56.3 | 34.8 | 17.5 | 108.0 | 28.3 |
| 10,000 | - | 10.5 | 56.7 | 24.4 | 56.3 | 89.3 | 28.0 | 280.6 | 27.2 |

Weights in metric tons

Percent of weight in the hatch and cover

*Lower limit of possible configuration rather than true minimum value

**Thickness of superconductor required is greater than 6.4 cm.

Table VII shows the weights calculated for the case without a passive shield. One can not merely subtract the hatch weight for some superconductor coils must be added. It was also found that the minimum weight did not always occur at the same value of wire size. Furthermore, the central hole was more important in the case of no hatch. In this case however, the weights were less than those for a sphere especially in the large sizes and at the high energy ranges. The comparison is shown in Figure 12. One notes that for large spacecraft the hatchless torus has a large weight advantage.

TABLE VII

Magnetic Shield Structure Weights-Torus Without Hatch

| Volume in cuft | R/r | Proton Energy in MEV | | | |
|-------------------|-----|----------------------|-------|-------|--------|
| | | 100 | 200 | 500 | 1000 |
| 100 | 8 | 2.1* | 3.7* | 8.4* | 23.8* |
| | 4 | 1.6* | 4.2* | 9.9* | 21.5* |
| | 2 | 1.7* | 6.4* | 16.1* | - ** |
| 1000 | 16 | 7.6 | 11.8 | 24.3* | 50.2* |
| | 8 | 5.1* | 8.0* | 16.8* | 40.6* |
| | 4 | 3.5* | 5.9* | 15.8* | 34.2* |
| | 2 | 5.0* | 10.1* | 22.8* | 76.0* |
| 10,000 | 16 | 20.8 | 30.5 | 59.8 | 114.2* |
| | 8 | 14.4 | 20.8 | 39.7* | 76.4* |
| | 4 | 10.2 | 14.3* | 31.7* | 64.8* |
| | 2 | 10.0* | 17.6* | 37.3* | 116.0* |

All weights in Metric Tons

*Lower limit of possible configuration rather than true minimum value

**Thickness of superconductor required is greater than 6.4 cm.

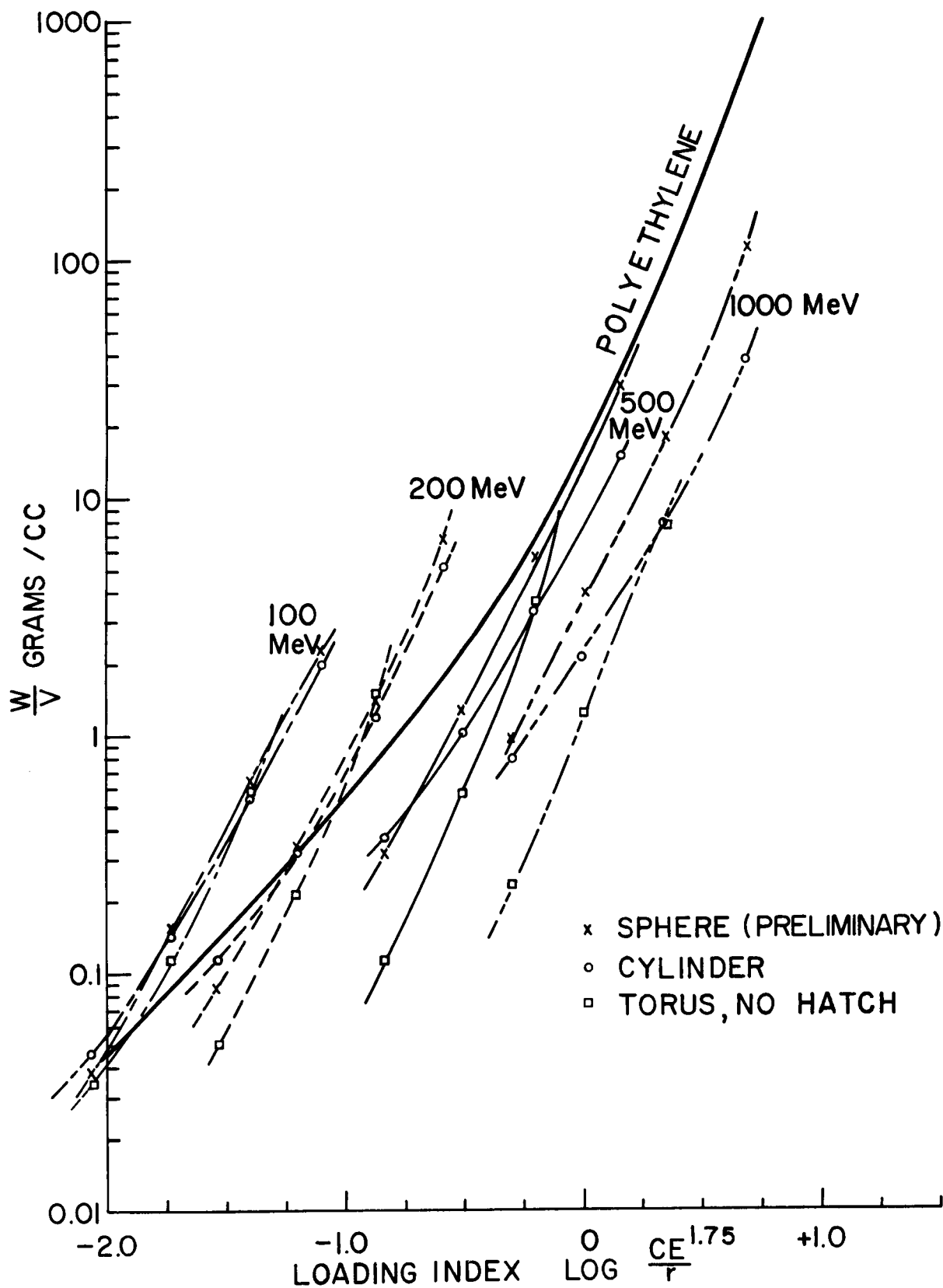


Figure 12. Comparison of Shielding Weights
II - Sphere, Cylinder, Torus, Polyethylene

4. Modular Configuration

For construction in space a craft should be made of units which can be easily assembled. The modules can be cylinders, spheres, cubes, etc. However, a ring of spheres can be shown to have the minimum structural weight. Thus, the weight of radiation shield has been calculated for three types of spherical modules shown in Figure 13. The central module has two openings which may be parallel to form a straight string of spheres or they may form a dihedral angle to form a ring of spheres. The blind end module has only one opening. The hatch end module has two openings with one having a passively shielded plug.

The weights were calculated for each type module and added to form a three-sphere spacecraft. Of course, the weight per unit volume can be computed just as before. The results are shown on Figure 14. Note that the modular type is lighter than the sphere or cylinder.

A type of spherical spacecraft that is different from that shown on Figure 7 has been used for Figure 14. By taking a combination of the blind end module and the hatch end module a single sphere has been formed. This removes the large protuberance from the end of Figure 7. By eliminating the thermal insulation at the axis where the superconducting coils meet, the need for the passive block is removed. In fact, the superconductor forms its own passive shield along the axis whereas the thermal insulation did not. Table VIII shows the required thickness of material at 8 grams/cc (assumed in place of Nb_3Sn) for each proton energy range treated. The depth of field is shown for minimum weight to be greater than the required depth.

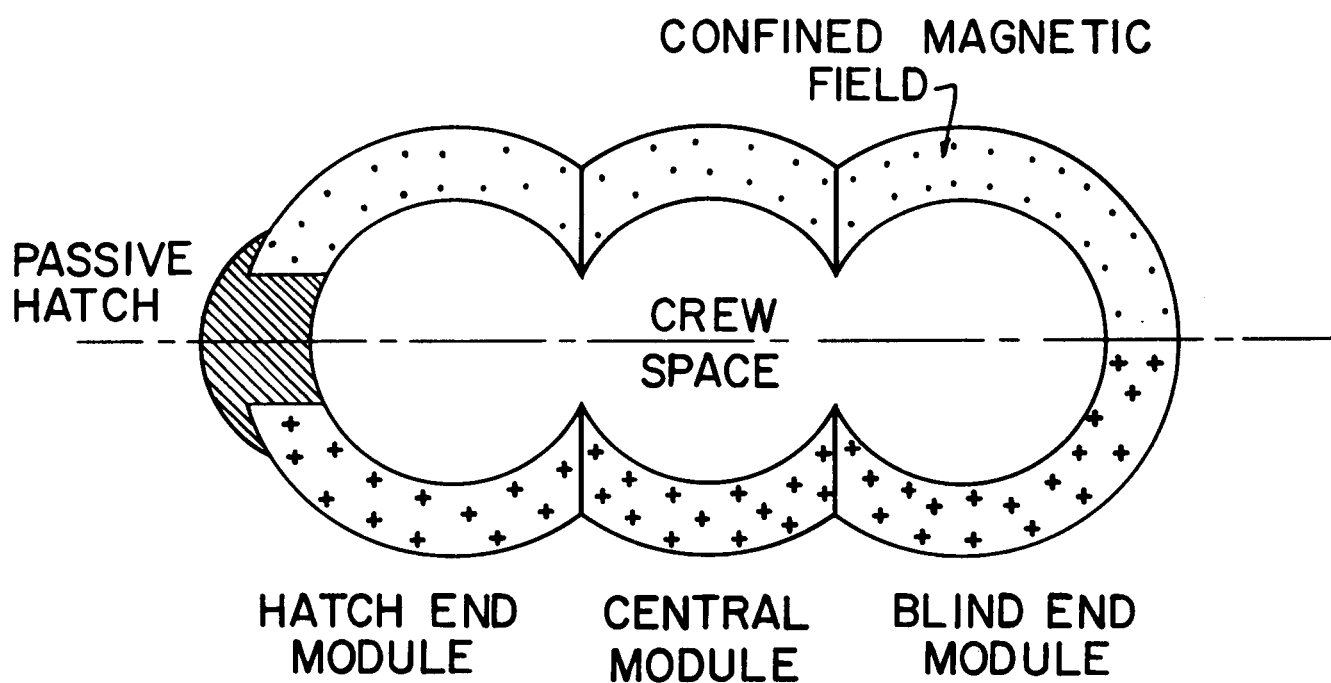


Figure 13. Schematic Diagram of Spherical Modules

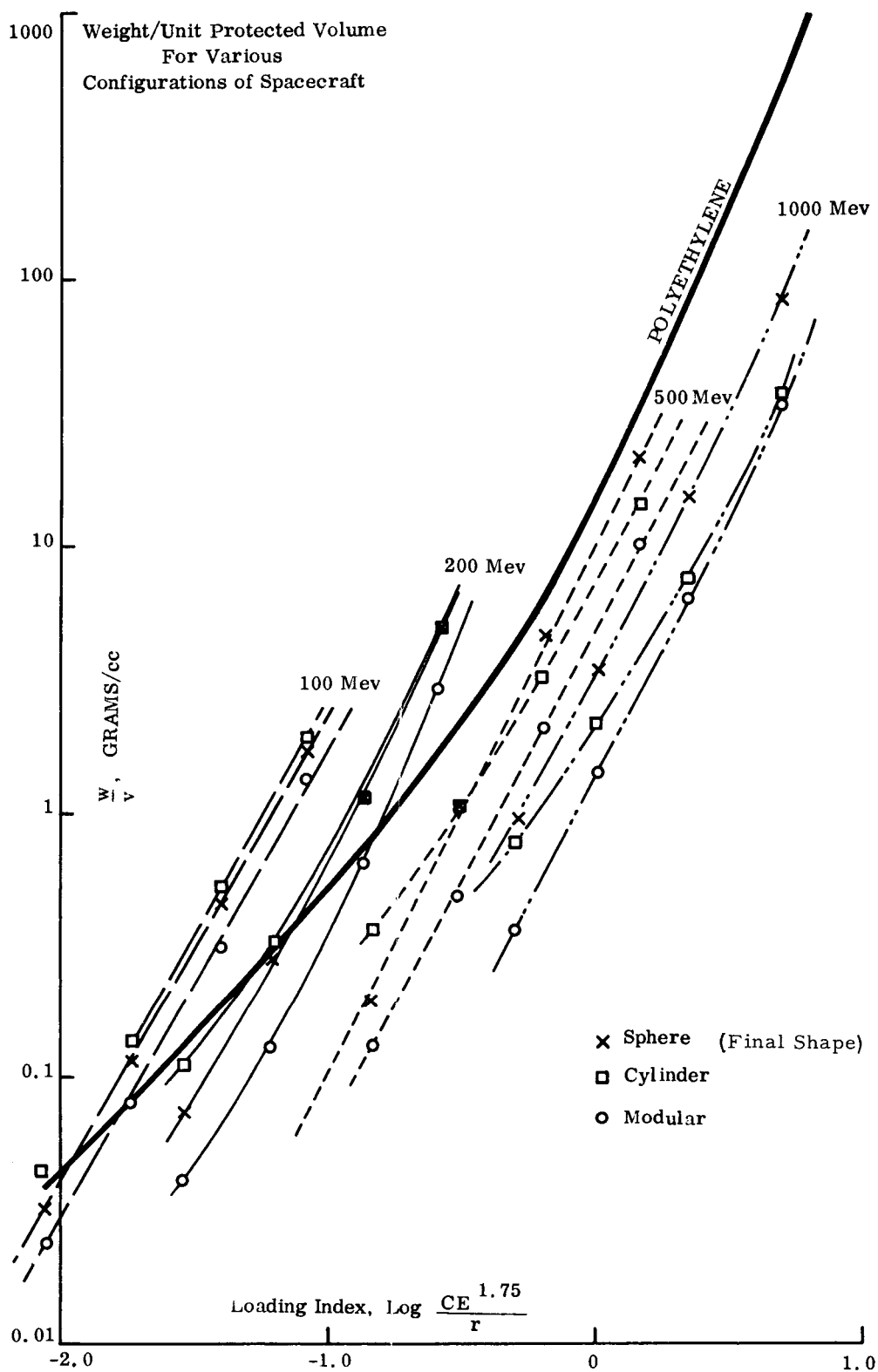


Figure 14. Comparison of Shielding Weights
III - Sphere, Cylinder, Module, Polyethylene

Table VIII

Wire Lengths & Stopping Power

| Proton Energy MeV | Stopping Power gm/cm ² | Thickness Required cm | Field Depth or Radial Wire Length in cm. | | | | cuft. Volume |
|----------------------|---|-----------------------------|---|-----|------|--------|--------------|
| | | | 10 | 100 | 1000 | 10,000 | |
| 100 | 11.7 | 1.46 | 31 | 59 | 136 | 198 | |
| 200 | 38.9 | 4.86 | 42 | 67 | 100 | 211 | |
| 500 | 170 | 21.2 | 36 | 58 | 86 | 176 | |
| 1000 | 480 | 58.8 | 64 | 64 | 94 | 189 | |

5. Unconfined Magnetic Field Configuration

The unconfined magnetic field can be used as shown in Section III to prevent protons from entering the crew space. Levy⁽¹¹⁾ has calculated the weights of shielding required. These weights were transposed for plotting against the Loading Index by Dow.⁽⁸⁾ Figure 15 shows these data plotted with the weight of a polyethylene shield. The active shields are indeed lighter than the passive shields for the high energy protons.

However, we find that the weights are still smaller for the confined field shields. The weights for the spherical configurations are shown to illustrate this point. The confined field weights fall to 30% of the unconfined field weights for high energy protons and large volumes.

C. Structural Weight

The structural weight was calculated according to the plan shown in Section III above. In the percentages shown on Table V one notes that the weights vary from 10 to 34% for the spherical shaped spacecraft. However,

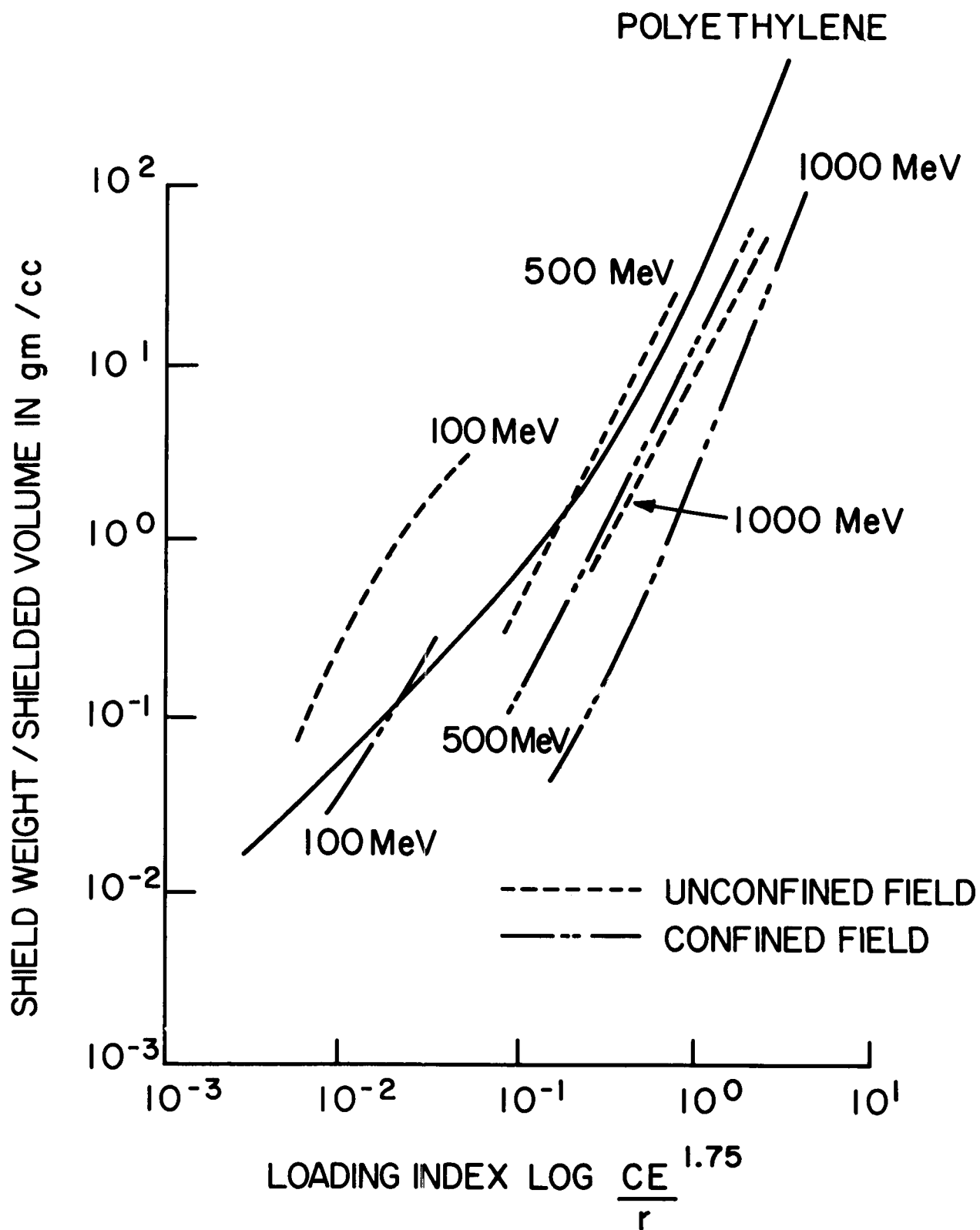


Figure 15. Comparison of Shielding Weights

IV - Confined vs. Unconfined Magnetic Fields

the magnitude of the structural weight increases with spacecraft volume and proton energy. By using the data for a spherical spacecraft, the data can be reduced to an empirical form

$$(10^4)(\text{structural weight}) = (\text{proton energy})^{4/3} (\sqrt{\text{volume}}). \quad (39)$$

This expression has no meaning except to show that a relatively simple relation could be derived if required.

D. Superconductor Wire Coils

According to the equations shown in Section III, the size of wire was computed that would be needed to produce the confined fields in each case. Given the cross section of wire (which could be made up of many single wires) and the area of the coil, the weights were computed separately for each spacecraft volume and proton energy. The results are shown on Table V as percentages. When the actual weights are examined, they increase with volume because the coils are somewhat a function of the surface area rather than the volume. Thus, the weight doubles between 10 and 100 cu. ft. of crewspace but then increases more slowly at 1000 and 10,000 cu. ft. This effect is compensated by the decrease in wire cross section as the size increases. In other words, the weight optimization for the whole spacecraft dictates that the shielding system shall be larger which means that the wire cross section may be smaller.

Nb_3Sn was chosen for the superconducting material because the BJ product is the highest in the working range. Other materials have lower

values for this product. Since NbZr is commercially available, calculations were made using it in place of Nb₃Sn. The value of BJ was taken as 7.5×10^8 (compared to 6×10^9 for Nb₃Sn) gauss amperes/cm². Results are shown in Table IX. The weight per unit volume are shown for the modular type of spacecraft and the values for Nb₃Sn are listed with the NbZr for comparison. The ratio lies between 2 and 3 to one in favor of the Nb₃Sn.

Table IX

Modular Type Spacecraft Weight/Unit Volume
Variation of Superconducting Wire
In grams/cc

| Proton Energy Superconductor Protected Space in Cu Ft | 100 | | 200 | | 500 | | 1000 MeV | |
|--|--------------------|------|--------------------|------|--------------------|------|--------------------|------|
| | Nb ₃ Sn | NbZr | Nb ₃ Sn | NbZr | Nb ₃ Sn | NbZr | Nb ₃ Sn | NbZr |
| 10 | 1.31 | 3.52 | 2.94 | 7.91 | 10.1 | 23.0 | 34.0 | 91.4 |
| 100 | 0.31 | 0.67 | 0.64 | 1.49 | 2.07 | 4.84 | 6.27 | 14.6 |
| 1000 | 0.08 | 0.15 | 0.16 | 0.31 | 0.48 | 0.97 | 1.40 | 2.75 |
| 10,000 | 0.02 | 0.04 | 0.04 | 0.06 | 0.13 | 0.22 | 0.36 | 0.61 |

E. Cost Calculations

Table VII shows the weight of shielding structure for the toroidal and spherical shaped spacecraft. The data show weights from two to two hundred metric tons. By any estimate the cost for this structure will be large. Therefore, we have calculated some approximate material costs.

During the machine calculations of the weights, the individual weights of superconductor, insulation, structure, and end caps were printed out as well as the total weight. When one examines these figures, the superconductor weight is found to be a large portion of the total (15 to 65%). Thus, the cost of the structure will be heavily dependent upon the cost of the superconductor since it is the most expensive. Quotations were solicited from vendors of superconducting materials in wire form. Selling prices were obtained on NbZr in several sizes since it is commercially available. Only one price was received for Nb₃Sn and it was 3 times that for NbZr.

The total estimated cost was calculated using $.74 \times 10^6$ \$/metric ton (330 \$/lb) for the superconductor (NbZr), 2.2 \$/kilogram (1 \$/lb) for the supporting structure, and 1.1 \$/kilogram (50 ¢/lb) for the insulation. A toroidal spacecraft configuration without hatch was chosen for computation, since that has been shown to be the lightest spacecraft. The calculated numbers are given in Table X. Since the price of superconducting materials will undoubtedly decrease, the costs are also shown for the cases in which the NbZr would be 10% and 5% of the present price. The costs are high in any case, However, to have a comparison, the cost of a polyethylene shield has also been computed. The

present quoted price varies depending upon the density, filler, form, color, purity, etc. For this calculation a price of 700 \$/metric ton (32 ¢/lb) was chosen. The weight of polyethylene required was obtained from the data used for Figure 11.

TABLE X

Material Cost - Weight Relations for Toroidal Configuration without a Hatch

| Crewspace Shield Proton Energy MEV | 100 Cu. ft. | | | | 1000 Cu. ft. | | | | 10,000 Cu. ft. | | | |
|---|-------------|--------|---------|------|--------------|---------|---------|------|----------------|---------|---------|------|
| | active | | passive | | active | | passive | | active | | passive | |
| | wt. | cost | wt. | cost | wt. | cost | wt. | cost | wt. | cost | wt. | cost |
| 100 | 1.6 | | .53 | | 3.5 | | 2.4 | | 10.2 | | 10.9 | |
| present | | 580. | | .37 | | 650. | | 1.6 | | 1,206. | | 7.6 |
| @10% | | 59. | | | | 69. | | | | 132. | | |
| @ 5% | | 30. | | | | 37. | | | | 73. | | |
| 200 | 4.2 | | 2.06 | | 5.9 | | 8.6 | | 14.3 | | 37.9 | |
| present | | 1,981. | | 1.4 | | 1,347. | | 6.0 | | 1,487. | | 26.5 |
| @10% | | 201. | | | | 141. | | | | 162. | | |
| @ 5% | | 102. | | | | 68. | | | | 94. | | |
| 500 | 9.9 | | 21.2 | | 15.8 | | 62.8 | | 31.7 | | 230 | |
| present | | 4,500. | | 14. | | 4,800. | | 44. | | 5,470. | | 161. |
| @10% | | 457. | | | | 496. | | | | 590. | | |
| @ 5% | | 233. | | | | 258. | | | | 319. | | |
| 1000 | 21.5 | | -- | | 34.2 | | 470 | | 64.8 | | 1200 | |
| present | | 9,570. | | -- | | 10,400. | | 329. | | 11,600. | | 840. |
| @10% | | 975. | | | | 1,080. | | | | 1,253. | | |
| @ 5% | | 497. | | | | 562. | | | | 678. | | |

Notes: Active - Confined Space Magnetic Field Shielding
 Passive - Polyethylene Shielding @ 700 \$/metric ton
 Weight - Metric tons
 Cost - Thousands of dollars
 present-NbZr @ $.74 \times 10^6$ \$/metric ton
 @10% -NbZr @ $.074 \times 10^6$ \$/metric ton
 @ 5% -NbZr @ $.037 \times 10^6$ \$/metric ton
 (Cost of structure and thermal insulation less than 1% of total cost)

V. PASSIVE SHIELDING

A. Introduction

A fundamental unknown in the passive shielding of radiation in space is the poorly-understood physics of the penetration of incident cosmic-ray particles in the shield. For incident particles whose range is shorter than the nuclear interaction mean free path, electromagnetic interactions dominate inside the shield; this case is relatively well understood today. In all other cases, however, nuclear interactions or chains of nuclear interactions (nuclear cascade) intervene. When this occurs, the incident proton generally no longer retains its identity on passing through the shield. Instead, it gives rise to a host of secondaries (neutrons, protons, pions, gamma rays, etc.), some of which will manage to emerge from the shield and do biological harm. In order to know the intensity of these secondaries emerging from shields of various thicknesses it is necessary to study the nuclear interactions and the nuclear cascade taking place in the shield.

During the period of this contract, our study of passive shielding advanced mainly in the following two respects:

(1) the raw experimental data from nuclear-cascade experiments conducted at the Brookhaven Cosmotron using 1 and 3 GeV protons were analysed from the point of view of passive shielding and depth dosimetry. Some preliminary results were reported by Shen.⁹

(2) The overall physics of passive shielding was examined from a fundamental and long-range standpoint. This study culminated in a special

report dated June 1963.²⁷ Summaries of these reports are given here.

These experiments are also of interest to the physics of the passage of high-energy particles through matter and to the various "thick-target" situations in astrophysics; these questions are, however, outside the scope of the present report. We are only interested here in applications to shielding. Experiments can be of use to shielding in two ways:

(a) They supply data which can be directly applied to the design of a shield made of the same absorber material as used in the experiments and bombarded by cosmic rays of energy similar to the energy used in the experiments.

(b) They supply data which can be compared with the predictions of shield calculations, thereby verifying or not verifying these calculations.

In the long run (b) is the more important for the ultimate and complete solution of the passive shielding problem. Already, a number of shielding calculations which take into account the nuclear cascade produced in the shield have been or are being undertaken (e. g. Ref. 33). It is generally recognized that calculations of this kind are very difficult to make at present. This is because we have very limited knowledge of the input information which must go into these calculations. It is therefore of interest to know whether shield calculations agree with experiments. If now or in the future it turns out that the theoretical calculations make fairly satisfactory predictions of experiment results, then these same calculational schemes can be used

with confidence in the design of shields not amenable to experimental testing. It may be recalled that since our knowledge of the radiobiological effects of radiation and of the incident cosmic-ray flux is quite uncertain, these shield calculations need not be very accurate to be useful in shield design.

B. Nuclear Cascade Experiments

There now have taken place at the Brookhaven Cosmotron a total of five nuclear-cascade experiments. Table XI lists some of the irradiation conditions of interest. It is to be noted that the absorbers used (called targets in the table) varies from Plexiglass (a material of low mass number) to iron (a material of mass number 56). Chondrite, which is probably similar to material on the lunar surface, may be considered to be aluminum for many shielding purposes. Figure 16 shows a typical target assembly used in the irradiations. The incident protons impinge on the center of the target face. The activation foils sandwiched inside the target detect the flux of various types of particles at various depths.

Our preliminary experimental data are summarized in Figure 17. The abscissa shows the depth in the shield measured in g/cm^2 . The ordinate gives the number of particles of types "N" and "n" (per incident primary) crossing the depth in question. Here "N" stands for all protons, neutrons, and charged pions above 50 MeV, whereas "n" stands for neutrons between 7 and 20 MeV. The incident energy and the shield material are given as the curve labels. It is seen that all the curves rise at first with depth, go

TABLE XI

Nuclear Cascade Experiments*

| Date | Proton Energy (GeV) | Target Material | Target Cross Section (cm x cm) | Target Thickness (g/cm ²) | Irradiation Time (min) | Monitoring Reaction | Integrated Flux (10 ¹³ protons) |
|----------|---------------------------|--------------------|--------------------------------------|---|------------------------------|------------------------------------|--|
| 2/10/61 | 3 | iron | 30.5 x 30.5 | 703 | 88 | Fe(\bar{p} , X)Ar ³⁷ | 1.0 \pm 0.1 |
| 6/6/62 | 1 | iron | 30.5 x 30.5 | 740 | 72 | Al(\bar{p} , X)Na ²⁴ | 7.56 \pm 0.10 |
| 20/11/62 | 1 | chondrite | 20.3 x 20.5 | 118 | 19 | " | 1.8 \pm 0.1 |
| 20/11/62 | 1 | plexiglass | 30.5 x 30.5 | 30.5 | 10 | " | 0.79 \pm 0.01 |
| 5/2/63 | 3 | chondrite | 45.7 x 45.7 | 263 | 150 | " | 2.14 |

* These experiments were part of a New York University series designed to study the basic physics of the nuclear cascade in condensed matter.

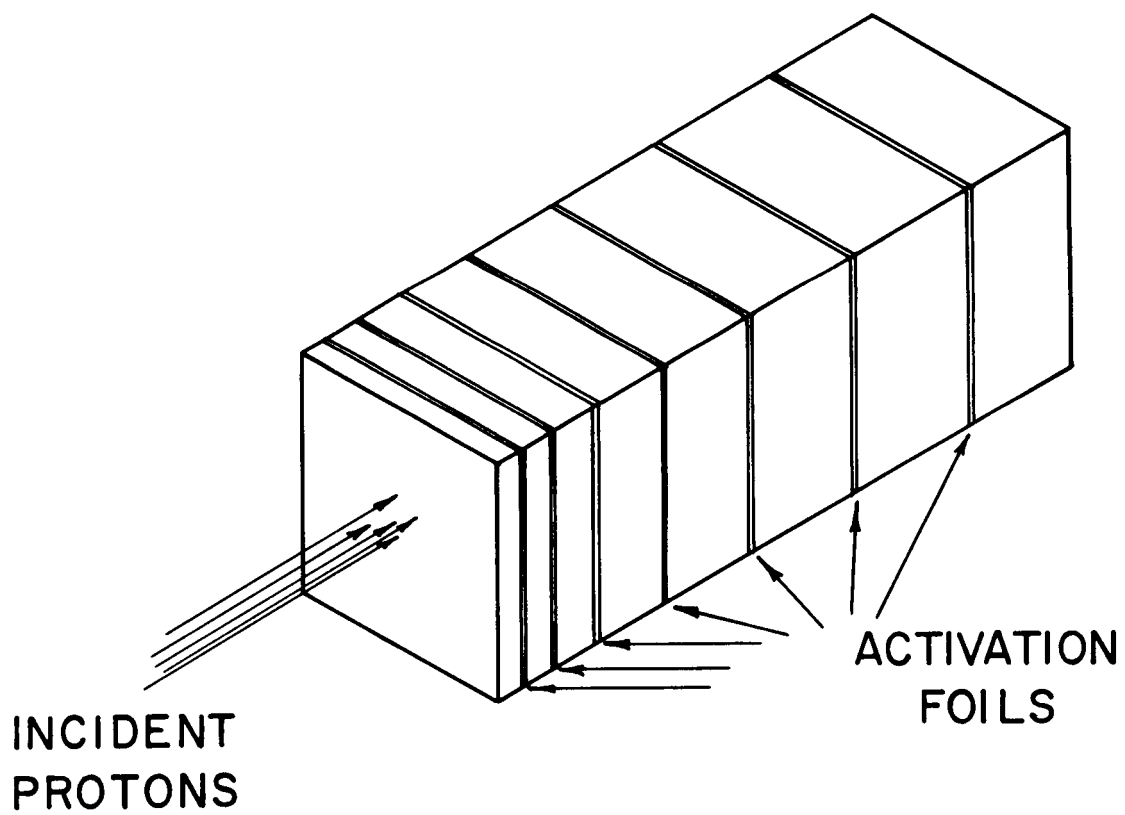


Figure 16. Typical Target Assembly

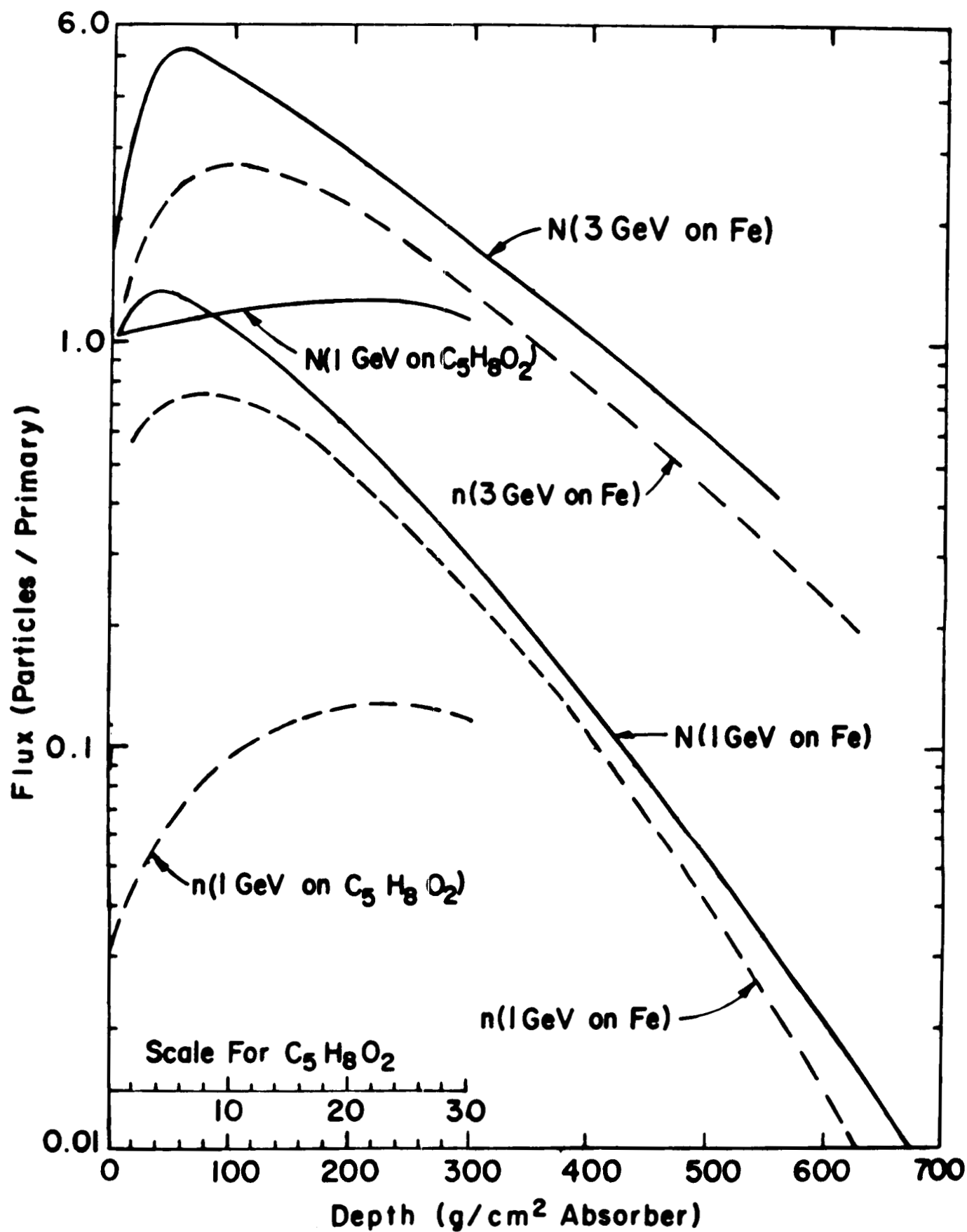


Figure 17. Transition Curves for the Fluxes of "N" and "n"

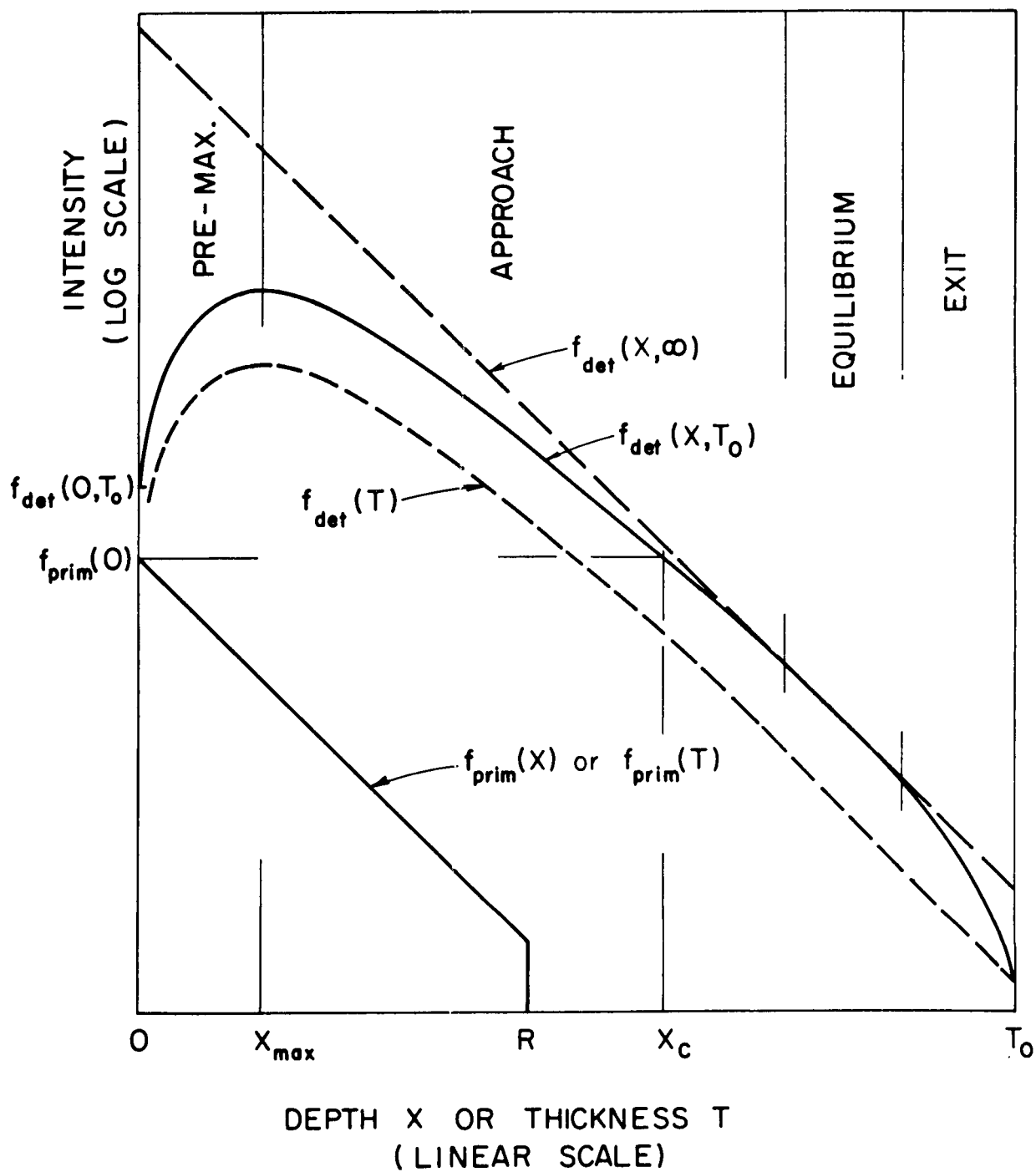


Figure 18. Some Idealized Transition Curves

The data from the experiments listed in Table XI will continue to be analysed in a more detailed and thorough manner than the initial analysis on which the curves in Fig. 17 were based. These newer results will be available later.

We feel that the nuclear cascade data taken at 1 and 3 GeV has been sufficiently studied to allow interpolation for incident energies lying anywhere between 1 and 3 GeV and for shield material having mass number between 10 and 60 atomic mass units.

C. Qualitative Cascade Description

As an incident particle strikes and travels through a target material, it collides with atomic nuclei and produces several new particles some of which also have nuclear collisions. This amplifying process is called a nuclear cascade. For convenience in this discussion, the secondaries from nuclear interactions are classified in Table XII, and an idealized sketch is shown in Figure 19. We have assumed a three GeV proton to be incident upon a thick condensed material, so that a cascade in a thinner target could be represented by cutting off the development at the thickness desired. A more complete description of the nuclear cascade follows.

Evaporation stars are represented in Figure 19 by the smaller circular symbols, magnified in the middle inset. Stars from which the only emerging secondaries are \leq ten MeV/nucleon particles (or, roughly, evaporation particles) are called evaporation stars. Stars from which the emerging secondaries contain not only evaporation particles but also \geq ten MeV/

TABLE XII

Classification of Secondaries from Inelastic Nuclear Interactions*

| Particle | Non-Interacting Particles | Interacting Particles | Interacting Particles, Non-Penetrating | Interacting Particles, Penetrating |
|---------------|------------------------------|--------------------------|--|--|
| neutron | $< \text{a few MeV (n)}$ | $> \text{a few MeV}$ | $\text{a few} - 200 \text{ MeV (n)}$ | $> 200 \text{ MeV (N)}$ |
| proton | $< 400 \text{ MeV (p)}$ | $> 400 \text{ MeV}$ | $400 - 600 \text{ MeV (p)}$ | $> 600 \text{ MeV (P)}$ |
| positive pion | $< 300 \text{ MeV}(\pi^+)$ | $> 300 \text{ MeV}$ | $300 - 500 \text{ MeV}(\pi^+)$ | $> 500 \text{ MeV}(\pi^+)$ |
| negative pion | none | all | $0 - 500 \text{ MeV}(\pi^-)$ | $> 500 \text{ MeV}(\pi^-)$ |
| nuclei | all | none | none | none |

* The classification is for convenience of discussion. The numbers quoted are subject to change as improved data are available.

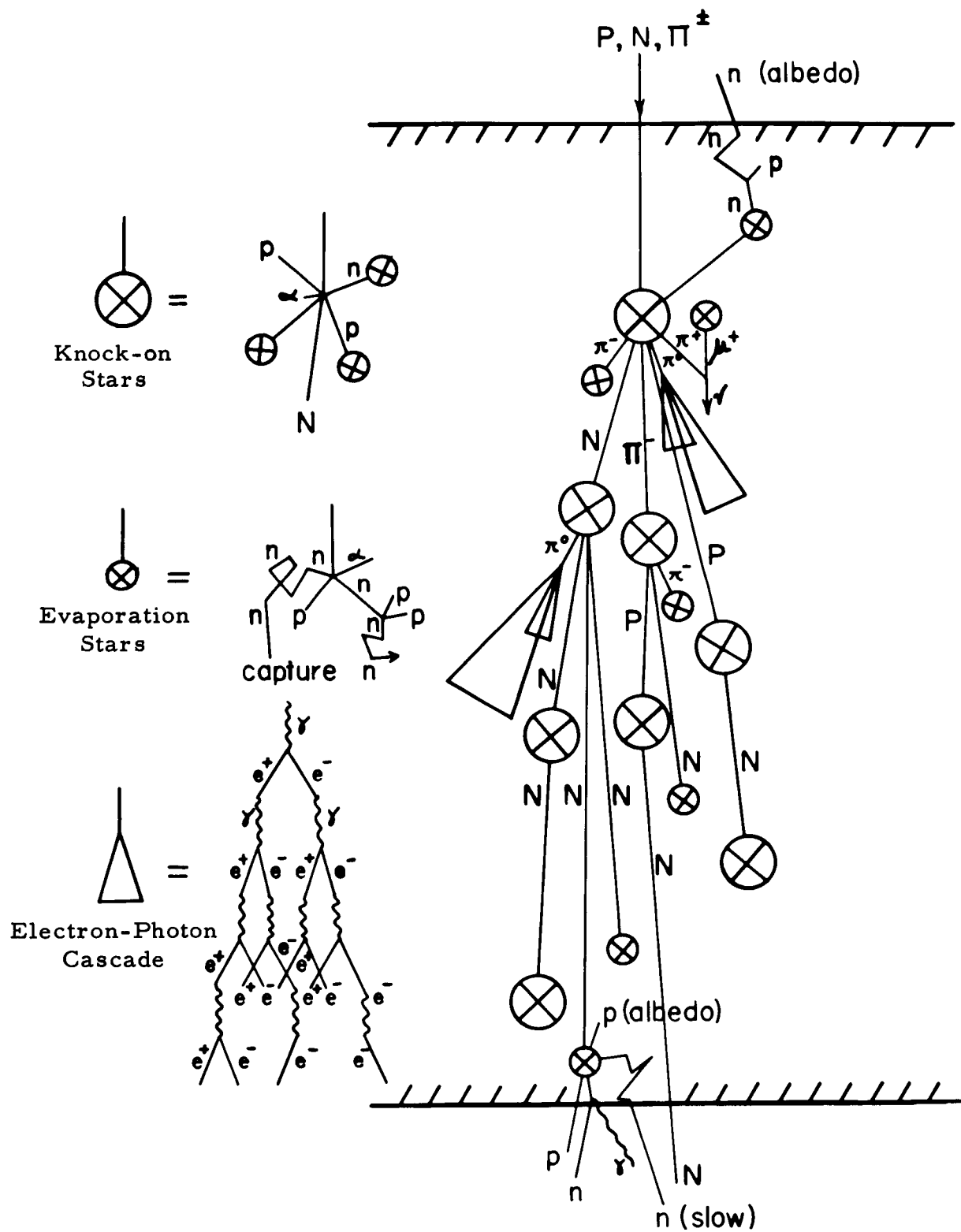


Figure 19. Schematic Representation of the Nuclear Cascade

nucleon particles (or, roughly speaking, knock-on particles) will be termed "knock-on stars." These stars are represented by the larger circular symbols, magnified in the upper inset. Each of these schematic insets merely shows an example of one of many types of individual stars. Obviously, secondaries from knock-on stars may produce further knock-on stars and evaporation stars, but secondaries from evaporation stars cannot make more knock-on stars. Knock-on stars in an emulsion are on the average initiated by particles above 100 MeV at least. For initiating particles above several hundred MeV, almost always one of the knock-on secondaries carries away a substantial fraction (e. g., one-half) of the initiating energy.

Some of the letter symbols used in Figure 19 have already been defined in the parentheses in Table XII; those not defined there have their usual meaning. Note that penetrating particles are all represented by capital letters (N, P, π^\pm).

Upon entering the absorber, the hypothetical 3-GeV proton will lose continually very small amounts of energy by ionization of the atoms along its straight path. At some depth in the absorber an inelastic nuclear interaction, which may be called the "first-generation star," will be induced in an absorber nucleus.

The non-interacting particles (see Table XII) from the first-generation star all slow down by ionization and stop at their respective ranges. In the process, they give up their kinetic energy to the absorber. If the absorber is tissue, this energy deposition is of biological interest. Penetrating particles (Table XII) are emitted (for this star, the "multiplicity" of

penetrating particles is $s = 3$: a neutron, a negative pion, and a proton). These will be called second-generation penetrating particles (the first-generation penetrating particle is the incident particle, i. e., the primary). As far as the ability to terminate in nuclear interaction is concerned, these three particles are on an equal footing. Thus, in an average distance equal to a nuclear mean free path, each of the three produces a knock-on star, as shown. We have drawn these three second-generation stars at different depths to emphasize the large fluctuations which actually occur.

One of the second-generation stars produces three third-generation penetrating particles ($s = 3$), all neutrons. Another second-generation star has $s = 2$. Still another has $s = 1$ only, perhaps because the proton initiating it has lost most of its original energy.

Among the seven third-generation stars induced by penetrating particles, three are knock-on stars, and four are evaporation stars. Only two of the seven have $s = 1$; the remainder have $s = 0$. Obviously, the original 3GeV have by now been widely shared. One of the two fourth-generation penetrating particles produces a fourth-generation star, surprisingly a knock-on star, but with $s = 0$. The other emerges from the absorber.

We have now traced the backbone of the nuclear cascade. We see that at first, pions (including those pions which are not penetrating particles) are produced; later, they are not. At first, the stars are knock-on stars; later, evaporation stars dominate. At first $s = 3$, and gradually s becomes zero. All these reflect the degradation of energy as the cascade develops.

More important is the fact that at first the penetrating particles are either neutrons, protons, or charged pions, but later only neutrons are penetrating particles. In other words, Figure 19 attempts to illustrate the fact that, at large depths, the nuclear cascade is propagated, and therefore controlled, by neutrons. This is a well known phenomenon in the shielding of high energy accelerators and in the cosmic ray cascade in the atmosphere, and has been discussed by Lindenbaum,²⁸ Wallace, et.al.,²⁹ Moyer,³⁰ and Peters³¹ among others. The reason for this phenomenon is that protons and charged pions are being produced at energies too low to permit them to undergo nuclear interaction with a long mean free path, i. e., to qualify as penetrating particles. One might guess the energy of most of these cascading neutrons. Obviously, they average above 200 MeV, for the production spectrum of knock-on neutrons is so steep that the majority of these neutrons must be near 200 MeV. The nuclear cascade is therefore propagated at large depths mainly by neutrons between, say, 200 and 300 MeV. Thus, at some depth x_N , the neutron dominance of penetrating particles is established; thereafter the cascade is propagated only by neutrons. At some other depth $x_{s=0}$, $s = 0$ is established for all stars; thereafter the existing penetrating particles one by one disappear upon nuclear interaction. Obviously both x_N and $x_{s=0}$ are larger for higher primary energy. Exactly how x_N and $x_{s=0}$ depend on primary energy (for a given shield material) is not well known.

The interacting particles which are not penetrating emerge from stars at large angles and interact with very short mean free paths; thus, they do not contribute significantly to the forward propagation of the cascade. The protons and pions among them will induce evaporation or knock-on stars. The neutrons (i. e., ≤ 200 MeV) among them have a more complicated fate. If produced at energy \geq ten MeV, these neutrons will in general induce evaporation stars (some of these will be low-energy nuclear reactions in which very few or no charged prongs are emitted), and these evaporation stars will, in turn emit evaporation neutrons of average energy near one MeV. If produced at energy \leq ten MeV, the neutrons will mainly undergo successive inelastic scatterings with shield nuclei, thus gradually losing energy by momentum transfer and by nuclear excitation. If the shield is thick enough, inelastic scatterings can bring the neutron down to about one MeV, but not much below this energy. Thus there will be found in the vicinity of any star shown in Figure 19 a number of neutrons of energy between one and ten MeV. Neutrons of such energy are usually called "fast neutrons," and have a high RBE. Slower neutrons would be biologically more palatable. But the only way these fast neutrons can slow down to below one MeV is by successive elastic scatterings with absorber nuclei. Classical mechanics tells us that the fractional energy loss (due to momentum transfer) by a neutron per elastic scattering is largest if the scattering absorber nucleus is the lightest, i. e., hydrogen. Thus, a shield containing some hydrogen (e. g., a hydrocarbon) would be more efficient

in slowing-down fast neutrons to a lower and hence biologically more acceptable energy. However, if the shield is very thin, little can be done about the fast neutrons.

The important thing to note here is that, as the penetrating particles bring the influence of the incident primary to various depths, they produce many stars along the way. These stars in turn give rise to a rich entourage of non-interacting particles, evaporation stars, fast and slow neutrons, electrons and photons; none of these can penetrate as far as the parent penetrating particles. Thus the penetrating particles control the cascade's average depth of penetration while all the other particles contribute to the opulence of the cascade at any particular depth.

As far as is known, the above qualitative description is consistent with all available experimental data.

VI. RESULTS AND CONCLUSIONS

The result of this year's work may be summarized as the following:

1. Protons in the range of 100-1,000 MeV were chosen as the most dangerous ionizing radiation in space that could be shielded. The Galactic cosmic rays have higher energy particles but the majority are much too high in energy to be shielded. Geomagnetically trapped radiations should be avoided by passing as rapidly as possible through them. Shielding from large solar flares is most economically done by remaining earthbound.
2. Particles in space are isotropic and shielding must be provided under these conditions.
3. Electromagnetic fields may be used to alter the particle trajectories.
 - a. Unconfined fields can be made that are lighter than passive shields, but they may subject the spacecraft crew to excessive magnetic fields. Even though considered to be zero, we calculated one case in which the field was 10^4 gauss.
 - b. Confined fields can be made that are lighter than passive shields, but cylindrical and spherical spacecraft will require a passively shielded hatch. Even with the hatch, the total shield weight is still less than that for a passive shield.
 - c. Confined field shields are lighter than unconfined field shields even with a hatch.
 - d. Confined fields may be used with toroidal spacecraft (without need for a passively shielded hatch) to produce a shielding system substantially

lighter than other types of shield.

e. Combinations of confined and unconfined shields may be made that will eliminate the need for a passively shielded hatch. Weight calculations have not been made for this case.

4. Of all parameters for optimization, weight was chosen as the most apropos. Size can be alleviated by modular construction when techniques for assembly in space are developed. Cost is delegated to the background in a conceptual study.

5. Four configurations of spacecraft were used for weight calculations: Spherical, cylindrical, toroidal, and spherical modular. Of these, modular has the smallest weight per unit volume of crewspace. The cylindrical shape has the next smallest for high energy protons and small volumes. These relations are shown in Figure 14.

6. Spherical and cylindrical spacecraft will require a passively shielded hatch. The toroidal spacecraft can be fabricated in sections which will preclude a hatch. When techniques for bonding superconducting wire are perfected, the toroidal spacecraft can use a mechanical hatch.

7. The hatch weights vary from 14 to 68% of the total for a spherical shape. Thus, a real saving can be obtained by eliminating the hatch. The weight per unit volume of crewspace is on Figure 12. At large volumes and high energies the gain from the elimination of the hatch is a factor of three.

8. All results were compared with total passive shields. For each configuration, the electromagnetic field systems are lighter than the polyethylene

shields for high energy particles. At low energy particles, only the large volumes have lighter fields.

9. Niobium tin superconducting wire will be lighter than niobium zirconium wire. Here the factor varies from two to three in favor of the niobium tin wire. However, the cost may rise by a factor of two.

10. Techniques for making superconducting wires must be advanced to provide the size of coils and bending techniques required for application to radiation shielding. Although NbZr could be used today, full potential of electromagnetic shielding cannot be realized until Nb₃Sn, or a more exotic alloy, can be obtained commercially.

11. Charging procedures for large superconducting coils must be developed that are safe from accident. With energy storage in the megajoule range, experience in handling these coils is mandatory.

12. Cryogenic apparatus is available for laboratory equipment. Large scale, portable closed cycle cryostats are not available. With time and development funds they may be produced since no new principle of operation is necessary.

13. The cost of an active shield was estimated to be larger than that of a passive shield. However, for high energy proton shielding and large spacecraft volumes, the costs would be comparable if the superconductor's price were reduced by a factor of ten or twenty.

14. Nuclear cascade experiments were made using 1 or 3 GeV protons. Targets of Fe, chondrites and plexiglass, were irradiated for measurements of shower fluxes at various depths. Close to the surface the flux increases

so that a critical depth may be found. If a shield is smaller than that depth, it would form an intensifier of damaging fluxes.

15. The shape of the flux-depth curve has been simplified to a curve that may be explained theoretically. No experimental data have been published to date which refute the theory proposed.

16. The overall physics of passive shielding was examined from a fundamental and long-range standpoint. A special report presents the status of the experimental data and theories of today.

VII. RECOMMENDATIONS

After this year's work the following recommendations can be made for future work.

1. Combinations of confined and unconfined electromagnetic fields should be studied to determine the weights of radiation shielding systems involved, the magnetic fields created in the crew space, and possibilities for transferring energy between the two source coils.
2. An operable model of a large size superconducting coil with self-contained cryogenic system should be designed and built to determine the feasibility and elucidate the compatibility problems.
3. Further experiments to measure nuclear cascades should be made using protons with energies between 100 and 1,000 MeV. Since these are the most dangerous and the most prevalent in solar flares, a knowledge of the effects of shielding (either active or passive) will be required before extraterrestrial trips are made that last more than several days.
4. Subsidiary tests on superconductors should be supported to show experimentally how to design large coils, to join wires without introducing resistance, to produce large currents in the coils, to make wires with large cross sections, and to support the coils against their own electromagnetic forces.
5. Nuclear cascade experiments made on superconducting coils and their supporting structure should be made to determine the number of secondaries produced. The extent of dosage would then be determinable.

Bibliography

1. F. B. McDonald, Solar Proton Manual, NASA, Goddard, Doc. No. X611-62-122, 1962.
2. T. Foesche, Current Estimates of Radiation Doses in Space, NASA, Langley, TND-1267, July, 1962.
3. J. W. Keller, Long Range NASA Shielding Requirements, Symp. Protection from Radiation Hazards in Space, Gatlinburg, Tenn., November, 1962.
4. F. S. Johnson, "Satellite Environment Handbook," Stanford Univ. Press, California, 1961.
5. L. F. Vosteen, Environmental Problems of Space Flight Structures, I. Ionizing Radiation in Space and Its Influence on Spacecraft Design, NASA, Langley, TND-1474, October, 1962.
6. W. L. Brown & J. D. Gabbe, The Electron Distribution in the Earth's Radiation Belts During July 1962 as Measured by Telstar, J. Geophys. Res., Vol. 68, No. 3 (1963), pg. 607.
7. K. Z. Morgan, Permissible Exposure to Ionizing Radiation, Science, Vol. 139, No. 3555, (1963), pg. 565.
8. N. F. Dow, S. P. Shen, & J. F. Heyda, Evaluations of Space Vehicle Shielding, T.I.S., R62SD31, Space Sciences Laboratory, General Electric Co., Phila., Pa.
9. S. P. Shen, Some Experiments on the Passage of High-Energy Protons

- in Dense Matter, Proc. Symp. on Prot. against Rad. Hazards in Space, TID7652 (1962) pg. 852.
10. G. V. Brown, Magnetic Radiation Shielding, NASA, Lewis Res. Ctr., Int. Conf. on High Intensity Mag. Fields, Cambridge, Mass., Nov., 1961.
 11. R. H. Levy, Radiation Shielding of Space Vehicles by Means of Superconducting Coils, AFBSD TN-61-7, April, 1961. (A. R. S. Jour., Nov. 1961, pg. 1568).
 12. C. Stoermer, The Polar Aurora, Clarendon Press, Oxford, 1955, pg. 209 ff.
 13. E. Fermi, Nuclear Physics, Rev. Ed., Univ. Chicago Press, Chicago (1950) pg. 224 ff.
 14. B. W. Roberts, Superconductive Materials and Some of Their Properties, Gen. Elec. Res. Lab. Report No. 63-RL-3252M, March, 1963.
 15. J. E. Kunzler, Superconductivity in High Magnetic Fields at High Current Densities, Rev. Mod. Phys., Vol. 33, No. 4 (1961) pg. 501-509.
 16. D. L. Martin, et al, A 101,000 Gauss Niobium-Tin Superconducting Solenoid, Gen. Elec. Res. Lab., Report. No. 63-RL-3397M, Aug. 1963.
 17. C. H. Rosner & H. W. Schadler, Relating Measurements on Short Superconducting Wires to Solenoid Performance, J. App. Phys., Vol. 34, No. 7, July 1963, pg. 2107.

18. C. H. Rosner, M. G. Benz, D. L. Martin, Coil Simultaneous Testing of Nb_3Sn , Wire Samples, J. App. Phys., Vol. 34, No. 7, July 1963, pg. 2108.
19. D. L. Martin, et al, A 100,000 Gauss Superconducting Solenoid, Gen. Elec. Res. Lab., Rept. No. 63-RL-3374M, June, 1963.
20. C. L. Kolbe & C. H. Rosner, Processing and Superconducting Properties of Nb_3Sn Wires, Gen. Elec. Res. Lab., Report. No. 62-RL-3153M, Oct. 1962.
21. R. W. Boom & R. S. Livingston, Superconducting Solenoids, Proc. IRE, March 1962, pg. 274.
22. J. E. Kunzler, et al, Superconductivity in Nb_3Sn at High Current Density in a Magnetic Field of 88 Gauss, Phys. Rev. Letters, Vol. 6, No. 3 (1961) pg. 89.
23. T. E. Hoffman, Reliable, Continuous, Closed-Circuit, 4 K Refrigeration for a Maser Application, Advances in Cryogenic Engineering, Vol. 8 Plenum Press, New York, 1963, pg. 203 ff.
24. S. H. Minnich, Protection of Superconducting Coils by Means of Damper Windings, Gen. Elec. Report, RS62GL165, Nov. 1962.
25. R. M. Sternheimer, Range-Energy Relations for Protons in Be, C, Al, Cu, Pb, and Au, Phys. Rev., Vol. 115, No. 1 (1959), page 137.
26. H. P. Furth, M. A. Levine, & R. W. Waniek, Production and Use of High Transient Magnetic Fields II, Rev. Sci. Instr., Vol. 28, No. 11 (1957), pg. 949-958.
27. S. P. Shen, Nuclear Problems in the Shielding and Dosimetry of Radiation in Space, Gen. Elec., Sp. Sci. Lab., Spec. Rept., June 1963.

28. S. J. Lindenbaum, Shielding of High Energy Accelerators, Ann. Rev. Nucl. Sci., Vol. 11 (1961), pg. 213.
29. R. Wallace, et al, Selected Topics in Radiation Dosimetry, pg. 579, Vienna, I. A. E. A. , 1961.
30. B. J. Moyer, Proc. First Inter. Symp. on Protection Near Large Accelerators, Saclay, Seine-et-Oise, Jan. 1962.
31. B. Peters, Handbook of Physics, Ed. E. U. Condon & H. Odishaw, McGraw-Hill, New York, (1958), pg. 9-201 ff.
32. A. F. Tooper, Electromagnetic Shielding Feasibility Study, ASD-TDR-63-194, May 1963.
33. _____, Neutron Physics Division Annual Progress Report for Period ending Sept. 1, 1962, Oak Ridge National Laboratory, Report No. ORNL 3360, Oct. 8, 1962, 322 pages.